Office de la Propriété Intellectuelle du Canada
Un organisme d'Industrie Canada

Canadian Intellectual Property Office
An agency of Industry Canada

CA 2786755 C 2017/06/20

(11)(21) **2 786 755**

(12) **BREVET CANADIEN**
CANADIAN PATENT

(13) **C**

(22) **Date de dépôt/Filing Date:** 2006/10/11
(41) **Mise à la disp. pub./Open to Public Insp.:** 2007/04/19
(45) **Date de délivrance/Issue Date:** 2017/06/20
(62) **Demande originale/Original Application:** 2 626 116
(30) **Priorité/Priority:** 2005/10/11 (US60/725,603)

(51) **Cl.Int./Int.Cl.** ***G01J 3/45*** (2006.01), ***G01J 3/44*** (2006.01), ***G01J 3/453*** (2006.01), *C12M 1/34* (2006.01)
(72) **Inventeurs/Inventors:**
WAX, ADAM, US;
PYHTILA, JOHN W., US

(73) **Propriétaire/Owner:**
DUKE UNIVERSITY, US

(74) **Agent:** BORDEN LADNER GERVAIS LLP

(54) **Titre : SYSTEMES ET PROCEDE ENDOSCOPIQUES D'INTERFEROMETRIE A FAIBLE COHERENCE ET A RESOLUTION ANGULAIRE**
(54) **Title: SYSTEMS AND METHOD FOR ENDOSCOPIC ANGLE-RESOLVED LOW COHERENCE INTERFEROMETRY**

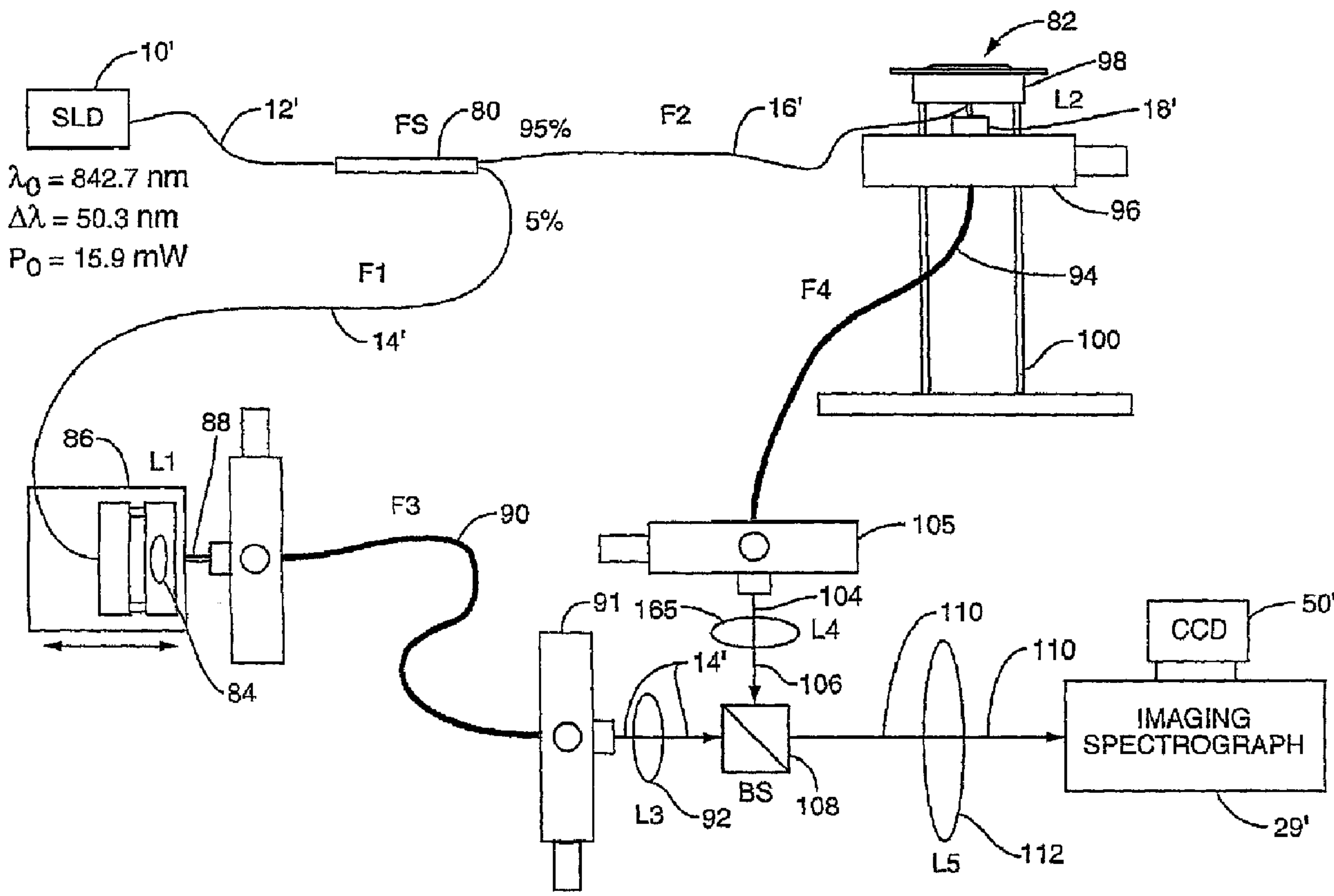

(57) **Abrégé/Abstract:**
Fourier domain a/LCI (faLCI) system and method which enables in vivo data acquisition at rapid rates using a single scan. Angle-resolved and depth- resolved spectra information is obtained with one scan. The reference arm can remain fixed with respect to the sample due to only one scan required. A reference signal and a reflected sample signal are cross-correlated and dispersed at a

(57) **Abrégé(suite)/Abstract(continued):**
multitude of reflected angles off of the sample, thereby representing reflections from a multitude of points on the sample at the same time in parallel. Information about all depths of the sample at each of the multitude of different points on the sample can be obtained with one scan on the order of approximately 40 milliseconds. From the spatial, cross-correlated reference signal, structural (size) information can also be obtained using techniques that allow size information of scatterers to be obtained from angle-resolved data.

ABSTRACT

Fourier domain a/LCI (faLCI) system and method which enables *in vivo* data acquisition at rapid rates using a single scan. Angle-resolved and depth-resolved spectra information is obtained with one scan. The reference arm can remain fixed with respect to the sample due to only one scan required. A reference signal and a reflected sample signal are cross-correlated and dispersed at a multitude of reflected angles off of the sample, thereby representing reflections from a multitude of points on the sample at the same time in parallel. Information about all depths of the sample at each of the multitude of different points on the sample can be obtained with one scan on the order of approximately 40 milliseconds. From the spatial, cross-correlated reference signal, structural (size) information can also be obtained using techniques that allow size information of scatterers to be obtained from angle-resolved data.

SYSTEMS AND METHOD FOR ENDOSCOPIC ANGLE-RESOLVED LOW COHERENCE INTERFEROMETRY

This application is a divisional application of co-pending application Serial No. 2,626,116 filed October 11, 2006.

Field of the Invention

[0003] Fourier domain angle-resolved low coherence interferometry (faLCI) system and method that enables data acquisition of angle-resolved and depth-resolved spectra information of a sample, in which depth and size information about the sample can be obtained with a single scan at rapid rates for *in vivo* applications in particular.

Background of the Invention

[0004] Examining the structural features of cells is essential for many clinical and laboratory studies. The most common tool used in the examination for the study of cells has been the microscope. Although microscope examination has led to great advances in understanding cells and their structure, it is inherently limited by the artifacts of preparation. The characteristics of the cells can only been seen at one moment in time with their structure features altered because of the addition of chemicals. Further, invasion is necessary to obtain the cell sample for examination.

[0005] Thus, light scattering spectrography (LSS) was developed to allow for in vivo examination applications, including cells. The LSS technique examines variations in the elastic scattering properties of cell organelles to infer their sizes and other dimensional information. In order to measure cellular features in tissues and other cellular structures, it is necessary to distinguish the singly scattered light from diffuse light, which has been multiply scattered and no longer carries easily accessible information about the scattering objects. This distinction or differentiation can be accomplished in several ways, such as the application of a polarization grating, by restricting or limiting studies and analysis to weakly scattering samples, or by using modeling to remove the diffuse component(s).

[0006] As an alternative approach for selectively detecting singly scattered light from sub-surface sites, low-coherence interferometry (LCI) has also been explored as a method of LSS. LCI utilizes a light source with low temporal coherence, such as broadband white light source for example. Interference is only achieved when the path length delays of the interferometer are matched with the coherence time of the light source. The axial resolution of the system is determined by the coherent length of the light source and is typically in the micrometer range suitable for the examination of tissue samples. Experimental results have shown that using a broadband light source and its second harmonic allows the recovery of information about elastic scattering using LCI. LCI has used time depth scans by moving the sample with respect to a reference arm directing the light source onto the sample to receive scattering information from a particular point on the sample. Thus, scan times were on the order of 5-30 minutes in order to completely scan the sample.

[0007] Angle-resolved LCI (a/LCI) has been developed as a means to obtain sub-surface structural information regarding the size of a cell. Light is split into a reference and sample beam, wherein the sample beam is projected onto the sample at different angles to examine the angular distribution of scattered light. The a/LCI technique combines the ability of (LCI) to detect singly scattered light from sub-surface sites with the capability of light scattering methods to obtain structural information with sub-wavelength precision and accuracy to construct depth-resolved tomographic images. Structural information is determined by examining the angular distribution of the back-scattered light using a single broadband light source is mixed with a reference field with an angle of propagation. The size distribution of the cell is determined by comparing the osciallary part of the measured angular distributions to predictions of Mie theory. Such a system is described in *Cellular Organization and Substructure Measured Using Angle-*

Resolved Low-Coherence Inteferometry, Biophysical Journal, 82, April 2002, 2256-2265.

[0008] The a/LCI technique has been successfully applied to measuring cellular morphology and to diagnosing intraepithelial neoplasia in an animal model of carcinogenesis. The inventors of the present application described such a system in *Determining nuclear morphology using an improved angle-resolved low coherence interferometry system* in Optics Express, 2003, 11(25): p. 3473-3484

The a/LCI method of obtaining structural information about a sample has been successfully applied to measuring cellular morphology in tissues and *in vitro* as well as diagnosing intraepithelial neoplasia and assessing the efficacy of chemopreventive agents in an animal model of carcinogenesis. a/LCI has been used to prospectively grade tissue samples without tissue processing, demonstrating the potential of the technique as a biomedical diagnostic.

[0009] Initial prototype and second generation a/LCI systems required 30 and 5 minutes respectively to obtain similar data. These earlier systems relied on time domain depth scans just as provided in previous LCI based systems. The length of the reference arm of the interferometer had to be mechanically adjusted to achieve serial scanning of the detected scattering angle. The method of obtaining angular specificity was achieved by causing the reference beam of the interferometry scheme to cross the detector plane at a variable angle. This general method for obtaining angle-resolved, depth-resolved backscattering distributions was disclosed in U.S. Patent No. 6,847,456 entitled "Methods and systems using field-based light scattering spectroscopy."

[0010] Other LCI prior systems are disclosed in U.S. Patent Nos. 6,002,480 and 6,501,551. U.S. Patent No. 6,002,480 covers obtaining depth-resolved spectroscopic distributions and discusses obtaining the size of scatterers by observing changes in wavelength due to elastic scattering properties. U.S. Patent No. 6,501,551 covers endoscopic application of interferometric imaging and does anticipate the use of Fourier domain concepts to obtain depth resolution. U.S. Patent No. 6,501,551 does not discuss measurement of angularly resolved scattering distributions, the use of scattered light to determine scatterer size by analysis of elastic scattering properties, nor the use of an imaging spectrometer to record data in parallel, whether that data is scattering or imaging data. Finally, U. S. Patent No. 7,061,622 discusses fiber optic means for measuring angular scattering distributions, but does not discuss the Fourier domain concept. Also because it describes an imaging technique, the embodiments all include focusing optics which limit the region probed.

Summary of the Invention

[0011] The present invention involves a new a/LCI technique called Fourier domain a/LCI (faLCI), which enables data acquisition at rapid rates using a single scan, sufficient to make *in vivo* applications feasible. The present invention obtains angle-resolved and depth-resolved spectra information about a sample, in which depth and size information about the sample can be obtained with a single scan, and wherein the reference arm can remain fixed with respect to the sample due to only one scan required. A reference signal and a reflected sample signal are cross-correlated and dispersed at a multitude of reflected angles off of the sample, thereby representing reflections from a multitude of points on the sample at the same time in parallel.

[0012] Since this angle-resolved, cross-correlated signal is spectrally dispersed, the new data acquisition scheme is significant as it permits data to be obtained in less than one second, a threshold determined to be necessary for acquiring data from *in vivo* tissues. Information about all depths of the sample at each of the multitude of different points on the sample can be obtained with one scan on the order of approximately 40 milliseconds. From the spatial, cross-correlated reference signal, structural (size) information can also be obtained using techniques that allow size information of scatterers to be obtained from angle-resolved data.

[0013] The faLCI technique of the present invention uses the Fourier domain concept to acquire depth resolved information. Signal-to-noise and commensurate reductions in data acquisition time are possible by recording the depth scan in the Fourier (or spectral) domain. The faLCI system combines the Fourier domain concept with the use of an imaging spectrograph to spectrally record the angular distribution in parallel. Thereafter, the depth-resolution of the present invention is achieved by Fourier transforming the spectrum of two mixed fields with the angle-resolved measurements obtained by locating the entrance slit of the imaging spectrograph in a Fourier transform plane to the sample. This converts the spectral information into depth-resolved information and the angular information into a transverse spatial distribution. The capabilities of faLCI have been initially demonstrated by extracting the size of polystyrene beads in a depth-resolved measurement.

[0014] Various mathematical techniques and methods are provided for determining size information of the sample using the angle-resolved, cross-correlated signal.

[0015] The present invention is not limited to any particular arrangement. In one embodiment, the apparatus is based on a modified Mach-Zehnder interferometer, wherein broadband light from a superluminescent diode is split into a reference beam and an input beam to the sample by a beamsplitter. In another embodiment, a unique optical fiber probe can be used to deliver light and collect the angular distribution of scattered light from the sample of interest.

[0016] The a/LCI method can be a clinically viable method for assessing tissue health without the need for tissue extraction via biopsy or subsequent histopathological evaluation. The a/LCI system can be applied for a number of purposes: early detection and screening for dysplastic epithelial tissues, disease staging, monitoring of therapeutic action and guiding the clinician to biopsy sites. The non-invasive, non-ionizing nature of the optical a/LCI probe means that it can be applied frequently without adverse affect. The potential of a/LCI to provide rapid results will greatly enhance its widespread applicability for disease screening.

Brief Description of the Drawing Figures

[0017] The accompanying drawing figures incorporated in and forming a part of this specification illustrate several aspects of the invention, and together with the description serve to explain the principles of the invention.

[0018] Figure 1A is a schematic of one exemplary embodiment of the faLCI system employing Mach-Zehnder interferometer;

[0019] Figure 1B is an illustration showing the relationship of the detected scattering angle to slit of spectrograph in the interferometer arrangement of Figure 1A;

[0020] Figure 2 is a flowchart illustrating the steps performed by the interferometer apparatus to recover depth-resolved spatial cross-correlated information about the sample for analysis;

[0021] Figures 3A-D illustrate examples of faLCI data recovered in the spectral domain for an exemplary sample of polystyrene beads, comprising the total acquired signal (Figure 3A), the reference field intensity (Figure 3B), the signal field intensity (Figure 3C), and the extracted, cross-correlated signal between the reference and signal field intensities (Figure 3D);

[0022] Figure 4A is an illustration of the axial spatial cross-correlated function performed on the cross-correlated faLCI data illustrated in Figure 3D as a function of depth and angle;

[0023] Figure 4B is an illustration of an angular distribution plot of raw and filtered data regarding scattered sample signal intensity as a function of angle in order to recover size information about the sample;

[0024] Figure 5A is an illustration of the filtered angular distribution of the scattered sample signal intensity compared to the best fit Mie theory to determine size information about the sample;

[0025] Figure 5B is a Chi-squired minimization of size information about the sample to estimate the diameter of cells in the sample;

[0026] Figure 6 is a schematic of exemplary embodiment of the faLCI system employing an optical fiber probe;

[0027] Figure 7A is a cutaway view of an a/LCI fiber-optic probe tip that may be employed by the faLCI system illustrated in Figure 6;

[0028] Figure 7B illustrates the location of the fiber probe in the faLCI system illustrated in Figure 7A;

[0029] Figure 8A is an illustration of an alternative fiber-optic faLCI system that may be employed with the present invention;

[0030] Figure 8B is an illustration of sample illumination and scattered light collection with distal end of probe in the faLCI system illustrated in Figure 8B; and

[0031] Figure 8C is an illustration of an image of the illuminated distal end of probe of the faLCI system illustrated in Figure 8A.

Detailed Description of the Preferred Embodiments

[0032] The embodiments set forth below represent the necessary information to enable those skilled in the art to practice the invention and illustrate the best mode of practicing the invention. Upon reading the following description in light of the accompanying drawing figures, those skilled in the art will understand the concepts of the invention and will recognize applications of these concepts not particularly addressed herein. It should be understood that these concepts and applications fall within the scope of the disclosure and the accompanying claims.

[0033] The present invention involves a new a/LCI technique called Fourier domain a/LCI (faLCI), which enables data acquisition at rapid rates using a single scan, sufficient to make in vivo applications feasible. The present invention obtains angle-resolved and depth-resolved spectra information about a sample, in which depth and size information about the sample can be obtained with a single scan, and wherein the reference arm can remain fixed with respect to the sample due to only one scan required. A reference signal and a reflected sample signal are cross-correlated and dispersed at a multitude of reflected angles off of the sample, thereby representing reflections from a multitude of points on the sample at the same time in parallel.

[0034] Since this angle-resolved, cross-correlated signal is spectrally dispersed, the new data acquisition scheme is significant as it permits data to be obtained in less than one second, a threshold determined to be necessary for acquiring data from *in vivo* tissues. Information about all depths of the sample at each of the multitude of different points on the sample can be obtained with one scan on the order of approximately 40 milliseconds. From the spatial, cross-correlated reference signal, structural (size) information can also be obtained using techniques that allow size information of scatterers to be obtained from angle-resolved data.

[0035] The faLCI technique of the present invention uses the Fourier domain concept to acquire depth resolved information. Signal-to-noise and commensurate reductions in data acquisition time are possible by recording the depth scan in the Fourier (or spectral) domain. The faLCI system combines the Fourier domain concept with the use of an imaging spectrograph to spectrally record the angular distribution in parallel. Thereafter, the depth-resolution of the present invention is achieved by Fourier transforming the spectrum of two mixed fields with the angle-resolved measurements obtained by locating the entrance slit of the imaging spectrograph in a Fourier transform plane to the sample. This converts the spectral information into depth-resolved information and the angular information into a transverse spatial distribution. The capabilities of faLCI have been initially demonstrated by extracting the size of polystyrene beads in a depth-resolved measurement.

[0036] The key advances of the present invention can be broken down into three components: (1) new rapid data acquisition methods, (2) fiber probe designs, and (3) data analysis schemes. Thus, the present invention is described in this matter for convenience in its understanding.

[0037] An exemplary apparatus, as well as the steps involved in the process of obtaining angle and depth-resolved distribution data scattered from a sample, are also set forth in Figure 2. The faLCI scheme in accordance with one embodiment of the present invention is based on a modified Mach-Zehnder interferometer as illustrated in Figure 1A. Broadband light 10 from a superluminescent diode (SLD) 12 is directed by a mirror 13 (step 60 in Figure 2) and split into a reference beam 14 and an input beam 16 to a sample 18 by beamsplitter BS1 20 (step 62 in Figure 3). The output power of the SLD 12 may be 3 milliWatts, having a specification of λo=850 nm, $\Delta\lambda$=20 nm FWHM for example, providing sufficiently low coherence length to isolate scattering from a cell layer within tissue. The path length of the reference beam 14 is set by adjusting retroreflector RR 22, but remains fixed during measurement. The reference beam 14 is expanded using lenses L1 (24) and L2 (26) to create illumination (step 64 in Figure 2), which is uniform and collimated upon reaching a spectrograph slit 48 in an imaging spectrograph 29. For example, L1 may have a focal length of 1.5 centimeters, and L2 26 may have focal length of 15 centimeters.

[0038] Lenses L3 (31) and L4 (38) are arranged to produce a collimated pencil beam 30 incident on the sample 18 (step 66 in Figure 2). By displacing lens L4 (38) vertically relative to lens L3 (31), the input beam 30 is made to strike the sample at an angle of 0.10 radians relative to the optical axis. This arrangement allows the full angular aperture of lens L4 (38) to be used to collect scattered light 40 from the sample 18. Lens L4 (38) may have a focal length of 3.5 centimeters.

[0039] The light 40 scattered by the sample 18 is collected by lens L4 (32) and relayed by a *4f* imaging system comprised of lenses L5 (43) and L6 (44) such that the Fourier plane of lens L4 (32) is reproduced in phase and amplitude at the spectrograph slit 48 (step 68 in Figure 2). The scattered light 40 is mixed with the reference field 14 at a second beamsplitter BS2 42 with the combined fields 46 falling upon the entrance slit (illustrated in Figure 1B as element 48) to the imaging spectrograph 29 (step 70 in Figure 2). The imaging spectrograph 29 may be the model SP2150i, manufactured by Acton Research for example. Figure 1B illustrates the distribution of scattering angle across the dimension of the slit 48. The mixed fields are dispersed with a high resolution grating (e.g. 1200 l/mm) and detected using a cooled CCD 50 (e.g. 1340 X 400, 20 μm X 20 μm pixels, Spec10:400, manufactured by Princeton Instruments) (step 72 in Figure 2).

[0040] The detected signal 46 is a function of vertical position on the spectrograph slit 48, *y*, and wavelength λ once the light is dispersed by the spectrograph 29. The detected signal at pixel (m, n) can be related to the signal 40 and reference fields 16 (E_s, E_r) as:

$$I(\lambda_m, y_n) = \left\langle \left| E_r(\lambda_m, y_n) \right|^2 \right\rangle + \left\langle \left| E_s(\lambda_m, y_n) \right|^2 \right\rangle + 2\,\mathrm{Re}\left\langle E_s(\lambda_m, y_n) E_r^*(\lambda_m, y_n) \right\rangle \cos\phi, \qquad (1)$$

where ϕ is the phase difference between the two fields 30, 16 and $\langle \cdots \rangle$ denotes an ensemble average in time. The interference term is extracted by measuring the intensity of the signal 30 and reference beams 16 independently and subtracting them from the total intensity.

[0041] In order to obtain depth resolved information, the wavelength spectrum at each scattering angle is interpolated into a wavenumber (k = 2 π / λ) spectrum and Fourier transformed to give a spatial cross correlation, $\Gamma_{SR}(z)$ for each vertical pixel y_n:

$$\Gamma_{SR}(z, y_n) = \int dk\, e^{ikz} \left\langle E_s(k, y_n) E_r^*(k, y_n) \right\rangle \cos\phi. \qquad (2)$$

The reference field 14 takes the form:

$$E_r(k) = E_o \exp\left[-((k-k_o)/\Delta k)^2\right]\exp\left[-((y-y_o)/\Delta y)^2\right]\exp[ik\Delta l] \tag{3}$$

where k_o (y_o and Δk (Δy) represent the center and width of the Gaussian wavevector (spatial) distribution and Δl is the selected path length difference. The scattered field 40 takes the form

$$E_s(k,\theta) = \sum_j E_o \exp\left[-((k-k_o)/\Delta k)^2\right]\exp[ikl_j]S_j(k,\theta) \tag{4}$$

where S_j represents the amplitude distribution of the scattering originating from the jth interface, located at depth l_j. The angular distribution of the scattered field 40 is converted into a position distribution in the Fourier image plane of lens L4 through the relationship $y = f_4\,\theta$. For the pixel size of the CCD 50 (e.g. 20 μm), this yields an angular resolution (e.g. 0.57 mrad) and an expected angular range (e.g. 228 mrad.).

[0042] Inserting Eqs. (3) and (4) into Eq. (2) and noting the uniformity of the reference field 14 (*Δy >> slit height*) yields the spatial cross correlation at the nth vertical position on the detector 29:

$$\Gamma_{SR}(z,y_n) = \sum_j \int dk\left|E_o\right|^2 \exp\left[-2((k-k_o)/\Delta k)^2\right]\exp[ik(z-\Delta l+l_j)] \quad \times S_j(k,\theta_n = y_n/f_4)\cos\phi\,. \tag{5}$$

Evaluating this equation for a single interface yields:

$$\Gamma_{SR}(z,y_n) = \left|E_o\right|^2 \exp\left[-((z-\Delta l+l_j)\Delta k)^2/8\right]S_j(k_o,\theta_n = y_n/f_4)\cos\phi\,. \tag{6}$$

[0043] Here we have assumed that the scattering amplitude S does not vary appreciably over the bandwidth of the source light 12. This expression shows that we obtain a depth resolved profile of the scattering distribution 40 with each vertical pixel corresponding to a scattering angle.

[0044] Figure 3A below shows typical data representing the total detected intensity (Equation (1), above) of the sum of the reference field 16 and the field scattered 40 by a sample of polystyrene beads, in the frequency domain given as a function of wavelength and angle, given with respect to the backwards scattering direction. In an exemplary embodiment, this data was acquired in 40 milliseconds and records data over 186 mrad, approximately 85% of the expected range, with some loss of signal at higher angles.

[0045] Figures 3B and 3C illustrate the intensity of the reference and signal fields 14, 30 respectively. Upon subtraction of the signal and reference fields 14, 30 from the total detected intensity, the interference 46 between the two fields is realized as illustrated in Figure 3D. At each angle, interference data 46 are interpolated into k-space and Fourier transformed to give the angular depth resolved profiles of the sample 18 as illustrated in Figure 4A. The Fourier transform of the angle-resolved, cross correlated signal 46, which is the result of signal 40 scattered at a multitude of reflected angles off the sample 18 and obtained in the Fourier plane of lens L4 (38), produces depth-resolved information about the sample 18 as a function of angle and depth. This provides depth-resolved information about the sample 18. Because the angle-resolved, cross-correlated signal 46 is spectrally dispersed, the data acquisition permits data to be obtained in less than one second. Information about all depths of the sample 18 at each of the multitude of different points (i.e. angles) on the sample 18 can be obtained with one scan on the order of approximately 40 milliseconds. Normally, time domain based scanning is required to obtain information about all depths of a sample at a multitude of different points, thus requiring substantial time and movement of the reference arm with respect to the sample.

[0046] In the experiments that produced the depth-resolved profile of the sample 18 illustrated in Figure 4A, the sample 18 consists of polystyrene microspheres (e.g. n=1.59, 10.1 μm mean diameter, 8.9% variance, NIST certified, Duke Scientific) suspended in a mixture of 80% water and 20% glycerol (n=1.36) to provide neutral buoyancy. The solution was prepared to obtain a scattering length $l = 200$ μm. The sample is contained in a round well (8mm diameter, 1mm deep) behind a glass coverslip (thickness, $d \sim 170$ μm) (not shown). The sample beam 30 is incident on the sample 18 through the coverslip. The round trip thickness through the coverslip ($2\, n\, d = 2\ (1.5)\ (170\ \mu m) =$ 0.53 mm – see Figure 4A) shows the depth resolved capability of the approach. The data are ensemble averaged by integrating over one mean free path (MFP). The spatial average can enable a reduction of speckle when using low-coherence light to probe a scattering sample. To simplify the fitting procedure, the scattering distribution is low pass filtered to produce a smoother curve, with the cutoff frequency chosen to suppress spatial correlations on length scales above 16μm.

[0047] In addition to obtaining depth-resolved information about the sample 18, the scattering distribution data (i.e. a/LCI data) obtained from the sample 18 using the disclosed data acquisition scheme can also be used to make a size determination of the nucleus using the Mie theory. A scattering distribution 74 of the sample 18 is illustrated in Figure 4B as a contour plot. The raw scattered information 74 about the sample 18 is shown as a function of the signal field 30 and angle. A filtered curve is determined using the scattered data 74. Comparison of the filtered scattering distribution curve 76 (i.e. a representation of the scattered data 74) to the prediction of Mie theory (curve 78 in Figure 5A) enables a size determination to be made.

[0048] In order to fit the scattered data 76 to Mie theory, the a/LCI signals are processed to extract the oscillatory component which is characteristic of the nucleus size. The smoothed data 76 are fit to a low-order polynomial (4^{th} order was used for example herein, but later studies use a lower 2^{nd} order), which is then subtracted from the distribution 76 to remove the background trend. The resulting oscillatory component is then compared to a database of theoretical predictions obtained using Mie theory 78 from which the slowly varying features were similarly removed for analysis.

[0049] A direct comparison between the filtered a/LCI data 76 and Mie theory data 78 may not possible, as the chi-squared fitting algorithm tends to match the background slope rather than the characteristic oscillations. The calculated theoretical predictions include a Gaussian distribution of sizes characterized by a mean diameter (d) and standard deviation (δD) as well as a distribution of wavelengths, to accurately model the broad bandwidth source.

[0050] The best fit (Figure 5A) is determined by minimizing the Chi-squared between the data 76 and Mie theory (Figure 5B), yielding a size of 10.2 +/- 1.7 μm, in excellent agreement with the true size. The measurement error is larger than the variance of the bead size, most likely due to the limited range of angles recorded in the measurement.

[0051] As an alternative to processing the a/LCI data and comparing to Mie theory, there are several other approaches which could yield diagnostic information. These include analyzing the angular data using a Fourier transform to identify periodic oscillations characteristic of cell nuclei. The periodic oscillations can be correlated with nuclear size and thus will possess diagnostic value. Another approach to analyzing a/LCI data is to compare the data to a database of angular scattering distributions generated with finite element method (FEM) or T-Matrix calculations. Such calculations may offer superior analysis as there are not subject to the same limitations as Mie theory. For example, FEM or T-Matrix calculations can model non-spherical scatterers and scatterers with inclusions while Mie theory can only model homogenous spheres.

[0052] As an alternative embodiment, the present invention can also employ optical fibers to deliver and collect light from the sample of interest to use in the a/LCI system for endoscopic applications. This alternative embodiment is illustrated in Figure 6.

[0053] The fiber optic a/LCI scheme for this alternative embodiment makes use of the Fourier transform properties of a lens. This property states that when an object is placed in the front focal plane of a lens, the image at the conjugate image plane is the Fourier transform of that object. The Fourier transform of a spatial distribution (object or image) is given by the distribution of spatial frequencies, which is the representation of the image's information content in terms of cycles per mm. In an optical image of elastically scattered light, the wavelength retains its fixed, original value and the spatial frequency representation is simply a scaled version of the angular distribution of scattered light.

[0054] In the fiber optic a/LCI scheme, the angular distribution is captured by locating the distal end of the fiber bundle in a conjugate Fourier transform plane of the sample using a collecting lens. This angular distribution is then conveyed to the distal end of the fiber bundle where it is imaged using a 4f system onto the entrance slit of an imaging spectrograph. A beamsplitter is used to overlap the scattered field with a reference field prior to entering the slit so that low coherence interferometry can also be used to obtain depth resolved measurements.

[0055] Turning now to Figure 6, the fiber optic faLCI scheme is shown. Light 12' from a broadband light source 10' is split into a reference field 14' and a signal field 16' using a fiber splitter (FS) 80. A splitter ratio of 20:1 is chosen in one embodiment to direct more power to a sample 18' via the signal arm 82 as the light returned by the tissue is typically only a small fraction of the incident power.

[0056] Light in the reference fiber 14' emerges from fiber F1 and is collimated by lens L1 (84) which is mounted on a translation stage 86 to allow gross alignment of the reference arm path length. This path length is not scanned during operation but may be varied during alignment. A collimated beam 88 is arranged to be equal in dimension to the end 91 of fiber bundle F3 (90) so that the collimated beam 88 illuminates all fibers in F3 with equal intensity. The reference field 14' emerging from the distal tip of F3 (90) is collimated with lens L3 (92) in order to overlap with the scattered field conveyed by fiber F4 (94). In an alternative embodiment, light emerging from fiber F1 (14') is collimated then expanded using a lens system to produce a broad beam.

[0057] The scattered field is detected using a coherent fiber bundle. The scattered field is generated using light in the signal arm 82 which is directed toward the sample 18' of interest using lens L2 (98). As with the free space system, lens L2 (98) is displaced laterally from the center of single-mode fiber F2 such that a collimated beam is produced which is traveling at an angle relative to the optical axis The fact that the incident beam strikes the sample at an oblique angle is essential in separating the elastic scattering information from specular reflections. The light scattered by the sample 18' is collected by a fiber bundle consisting of an array of coherent single mode or multi-mode fibers. The distal tip of the fiber is maintained one focal length away from lens L2 (98) to image the angular distribution of scattered light. In the embodiment shown in Figure 6, the sample 18' is located in the front focal plane of lens L2 (98) using a mechanical mount 100. In the endoscope compatible probe shown in Figure 7, the sample is located in the front focal plane of lens L2 (98) using a transparent sheath (element 102).

[0058] As illustrated in Figure 6 and also Figure 7B, scattered light 104 emerging from a proximal end 105 of the fiber probe F4 (94) is recollimated by lens L4 (104) and overlapped with the reference field 14' using beamsplitter BS (108). The two combined fields 110 are re-imaged onto the slit (element 48' in Figure 7) of the imaging spectrograph 29' using lens L5 (112). The focal length of lens L5 (112) may be varied to optimally fill the slit 48'. The resulting optical signal contains information on each scattering angle across the vertical dimension of the slit 48' as described above for the apparatus of Figures 1A and 1B.

[0059] It is expected that the above-described a/LCI fiber-optic probe will collect the angular distribution over a 0.45 radian range (approx. 30 degrees) and will acquire the complete depth resolved scattering distribution 110 in a fraction of a second.

[0060] There are several possible schemes for creating the fiber probe which are the same from an optical engineering point of view. One possible implementation would be a linear array of single mode fibers in both the signal and reference arms. Alternatively, the reference arm 96 could be composed of an individual single mode fiber with the signal arm 82 consisting of either a coherent fiber bundle or linear fiber array.

[0061] The fiber probe tip can also have several implementations which are substantially equivalent. These would include the use of a drum or ball lens in place of lens L2 (98). A side-viewing probe could be created using a combination of a lens and a mirror or prism or through the use of a convex mirror to replace the lens-mirror combination. Finally, the entire probe can be made to rotate radially in order to provide a circumferential scan of the probed area.

[0062] Yet another data acquisition embodiment of the present invention could be a fa/LCI system is based on a modified Mach-Zehnder interferometer as illustrated in Figure 8A. The output 10'' from a fiber-coupled superluminescent diode (SLD) source 12'' (e.g. Superlum, $P_o = 15$ mW, $\lambda o = 841.5$ nm, $\Delta\lambda = 49.5$ nm, coherence length = 6.3 μm) is split into sample arm delivery fiber 16'' and a reference arm delivery fiber 14'' by a 90/10 fiber splitter FS (80') (e.g. manufactured by AC Photonics). The sample arm delivery fiber 16'' can consist of either of the following for example: (1) a single mode fiber with polarization control integrated at the tip; or (2) a polarization maintaining fiber. A sample probe 113 is assembled by affixing the delivery fiber 16''($NA \cong 0.12$) along the ferrule 114 at the distal end of a fiber bundle 116 such that the end face of the delivery fiber 16'' is parallel to and flush with the face of the fiber bundle 116. Ball lens L1 (115) (e.g. $f_l = 2.2$ mm) is positioned one focal length from the face of the probe 113 and centered on the fiber bundle 116, offsetting the delivery fiber 16'' from the optical axis of lens L1 (115). This configuration, which is also depicted in Figure 8B, produces a collimated beam 120 (e.g. P = 9 mW) with a diameter (e.g. $2f_1NA$) of 0.5 mm incident on the sample 18'' at an angle of 0.25 rad. for example.

[0063] The scattered light 122 from the sample is collected by lens L1 (115) and, via the Fourier transform property of the lens L1 (115, the angular distribution of the scattered field 122 is converted into a spatial distribution at the distal face of the multimode coherent fiber bundle 116 (e.g. Schott North America, Inc., length = 840 mm, pixel size = 8.2 µm, pixel count = 13.5K) which is located at the Fourier image plane of lens L1 (115). The relationship between vertical position on the fiber bundle, y', and scattering angle, θ is given by $y' = f_1\theta$. As an illustration, the optical path of light scattered 122 at three selected scattering angles is shown in Figure 8B. Overall, the angular distribution is sampled by approximately 130 individual fibers for example, across a vertical strip of the fiber bundle 116", as depicted by the highlighted area in Figure 8C. The 0.2 mm, for example, thick ferrule (d_1) separating the delivery fiber 16'' and fiber bundle 116 limits the minimum theoretical collection angle ($\theta_{\min,th} = d_1/f_1$) to 0.09 rad in this example. The maximum theoretical collection angle is determined by d_1 and d_2, the diameter of the fiber bundle, by $\theta_{\max,th} = (d_1 + d_2)/f_1$ to be 0.50 rad. Experiments using a standard scattering sample 122 indicate the usable angular range to be $\theta_{\min} = 0.12$ rad. to $\theta_{\max} = 0.45$ rad. d_1, for example, can be minimized by fabricating a channel in the distal ferrule 123 and positioning the delivery fiber 16'' in the channel. The fiber bundle 116 is spatially coherent, resulting in a reproduction of the collected angular scattering distribution at the proximal face. Additionally, as all fibers in the bundle 116 are path length matched to within the coherence length, the optical path length traveled by scattered light 122 at each angle is identical. The system disclosed in "Fiber-optic-bundle-based optical coherence tomography," by T. Q. Xie, D. Mukai, S. G. Guo, M. Brenner, and Z. P. Chen in *Optics Letters* 30(14), 1803-1805 (2005) (hereinafter "Xie"), discloses a multimode coherent fiber bundle into a time-domain optical coherence tomography system and demonstrated that the modes of light coupled into an individual fiber will travel different path lengths. In the example herein of the present invention, it was experimentally determined that the higher order modes are offset from the fundamental mode by 3.75 mm, well beyond the depth (~100 μm) required for gathering clinically relevant data. Additionally, the power in the higher order modes had a minimal affect on dynamic range as the sample arm power is significantly less than the reference arm power. Finally, it should be noted that while the system disclosed in Xie collected data serially through individual fibers, the example of the present invention herein uses 130 fibers to simultaneously collect scattered light across a range of angles in parallel, resulting in rapid data collection.

[0064] The angular distribution exiting a proximal end 124 of the fiber bundle 116 is relayed by the 4f imaging system of L2 and L3 ($f_2 = 3.0$ cm, $f_3 = 20.0$ cm) to the input slit 48'' of the imaging spectrograph 29'' (e.g. Acton Research, InSpectrum 150). The theoretical magnification of the 4f imaging system is (f_3/f_2) 6.67 in this example. Experimentally, the magnification was measured to be $M = 7.0$ in this example with the discrepancy most likely due to the position of the proximal face 124 of the fiber bundle 116 with relation to lens L2 (126). The resulting relationship between vertical position on the spectrograph slit 48'', y, and θ is $y = Mf_1(\theta - \theta_{\min})$. The optical path length of the reference arm is matched to that of the fundamental mode of the sample arm. Light 127 exiting the reference fiber 14'' is collimated by lens L4 (128) (e.g. f = 3.5 cm, spot size = 8.4 mm) to match the phase front curvature of the sample light and to produce even illumination across the slit 48'' of the imaging spectrograph 29''. A reference field 130 may be attenuated by a neutral density filter 132 and mixed with the angular scattering distribution at beamsplitter BS (134). The mixed fields 136 are dispersed with a high resolution grating (e.g. 1200 lines/mm) and detected using an integrated, cooled CCD (not shown) (e.g. 1024 x 252, 24 μm x 24 μm pixels, 0.1 nm resolution) covering a spectral range of 99 nm centered at 840 nm, for example.

[0065] The detected signal 136, a function of wavelength, λ, and θ, can be related to the signal and reference fields (*Es, Er*) as:

$$I(\lambda_m,\theta_n)=\left\langle\left|E_r(\lambda_m,\theta_n)\right|^2\right\rangle+\left\langle\left|E_s(\lambda_m,\theta_n)\right|^2\right\rangle+2\operatorname{Re}\left\langle E_s(\lambda_m,\theta_n)E_r^*(\lambda_m,\theta_n)\cos(\phi)\right\rangle, \quad (1)$$

where ϕ is the phase difference between the two fields, (m,n) denotes a pixel on the CCD, and $\langle\ldots\rangle$ denotes a temporal average. $I(\lambda_m, \theta_n)$ is uploaded to a PC using LabVIEW manufactured by National Instruments software and processed in 320 ms to produce a depth and angle resolved contour plot of scattered intensity. The processing of the angle-resolved scattered field to obtain depth and size information described above, and in particular reference to the data acquisition apparatus of Figures 1A and 1B, can then used to obtain angle-resolved, depth-resolved information about the sample 18'' using the scattered mixed field 136 generated by the apparatus in Figure 8.

[0066] The embodiments set forth above represent the necessary information to enable those skilled in the art to practice the invention and illustrate the best mode of practicing the invention. Upon reading the following description in light if the accompanying drawings figures, those skilled in the art will understand the concepts of the invention and will recognize applications of these concepts not particularly addressed herein. It should be understood that these concepts and applications fall within the scope of the disclosure.

[0067] Those skilled in the art will recognize improvements and modifications to the preferred embodiments of the present invention. All such improvements and modifications are considered within the scope of the concepts disclosed herein and the claims that follow.

CLAIMS:

1. A fiber optic probe for an apparatus for obtaining depth-resolved spectra of an in vivo sample for determining the structural characteristics of scatterers within the sample, the apparatus including a polarized light source configured to deliver polarized light through an optical fiber to a fiber splitter to split the light into a sample beam and a reference beam, the probe comprising:

a lens having an optical axis;

a single mode delivery fiber with polarization control integrated at a tip of the delivery fiber or a polarization maintaining fiber for carrying the sample beam and maintaining the polarization of the sample beam; and

a fiber bundle receiver comprised of a plurality of optical fibers having substantially matching path lengths and having a proximal end and a distal end forming a face, the face of the distal end of the fiber bundle receiver positioned at one focal length from the lens and centered in the optical axis;

wherein the delivery fiber is affixed to the distal end of, and disposed adjacent to the periphery of, the fiber bundle offset from the optical axis for directing the sample beam such that the sample beam travels from the delivery fiber through the lens displaced laterally from the end of the delivery fiber to provide a collimated beam incident on the sample at an oblique angle relative to the optical axis, and wherein the fiber bundle receiver is adapted to receive a scattered sample beam from the sample which is located at the other focus of the lens, such that the plurality of optical fibers receives an angular distribution of the scattered sample beam via a Fourier transform property of the lens.

2. The fiber optic probe of claim 1, wherein the plurality of optical fibers in the fiber bundle receiver are arranged to collect scattered light at a plurality of angles and simultaneously obtain the angular scattering distribution of the scattered sample beam.

3. The fiber optic probe of claim 1, wherein the plurality of optical fibers of the fiber bundle receiver comprises a linear array of single mode or multimode optical fibers.

4. The fiber optic probe of claim 1, wherein the plurality of optical fibers possess the same spatial arrangement at distal and proximal ends of the plurality of optical fibers of the fiber bundle receiver such that the plurality of optical fibers are spatially coherent with respect to conveying the angular scattering distribution of the scattered sample beam.

5. The fiber optic probe of claim 1 wherein the lens is comprised of a drum lens or a ball lens.

6. The fiber optic probe of claim 1, wherein the lens is configured to rotate radially about the optical axis to provide a circumferential scan of the sample.

7. The fiber optic probe of claim 1, further comprising a transparent sheath used to locate the sample at the one focal length from the lens.

8. The fiber optic probe of claim 1, wherein the plurality of fibers are configured to receive the angular distribution collected over a range of 30 degrees relative to the optical axis.

9. The fiber optic probe as claimed in any preceding claims 1 to 8 and further comprising a beamsplitter adapted to receive the reference beam and the angular scattering distribution of the scattered sample beam from the plurality of optical fibers, wherein the beamsplitter cross-correlates the sample beam and the reference beam to produce an angle-resolved cross-correlated signal.

10. The fiber optic probe of claim 9, further comprising an imaging spectrograph that spectrally disperses the -resolved cross-correlated angle-resolved signal to yield an angle-resolved, spectrally-resolved profile at each of the multitude of reflected angles in parallel at the same time.

11. The fiber optic probe of claim 10, further comprising a processor that receives the

angle-resolved, spectrally-resolved profile and Fourier transforms the profile to produce an angle-resolved depth resolved profile which is analyzed to determine the structural characteristics.

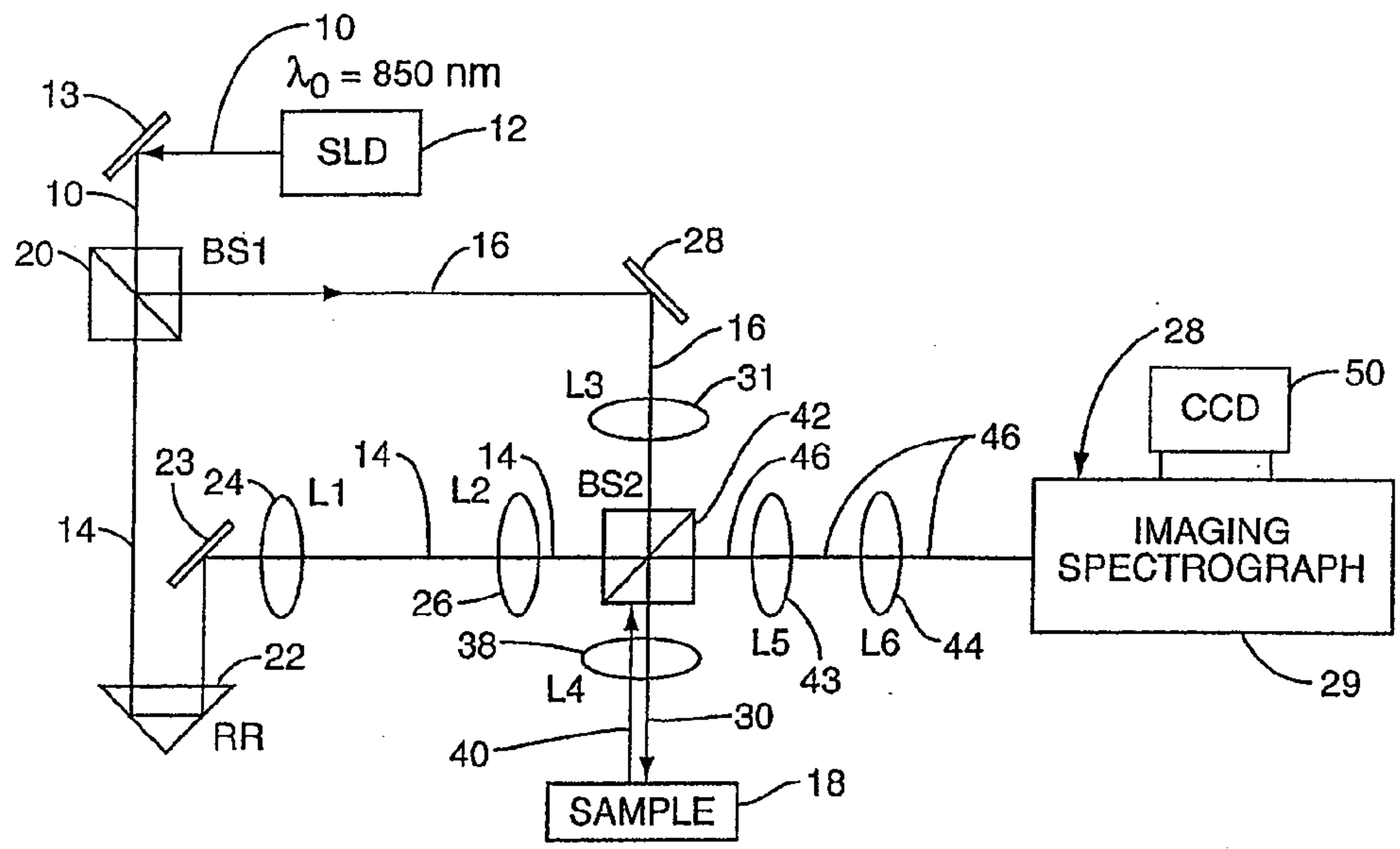
10
λ_0 = 850 nm
13
SLD
12
10
20
BS1
16
28
16
L3
31
42
46
46
28
CCD
50
23
24
L1
14
L2
14
BS2
14
IMAGING
SPECTROGRAPH
26
38
L4
L5
L6
44
43
29
22
RR
40
30
SAMPLE
18

FIG. 1A

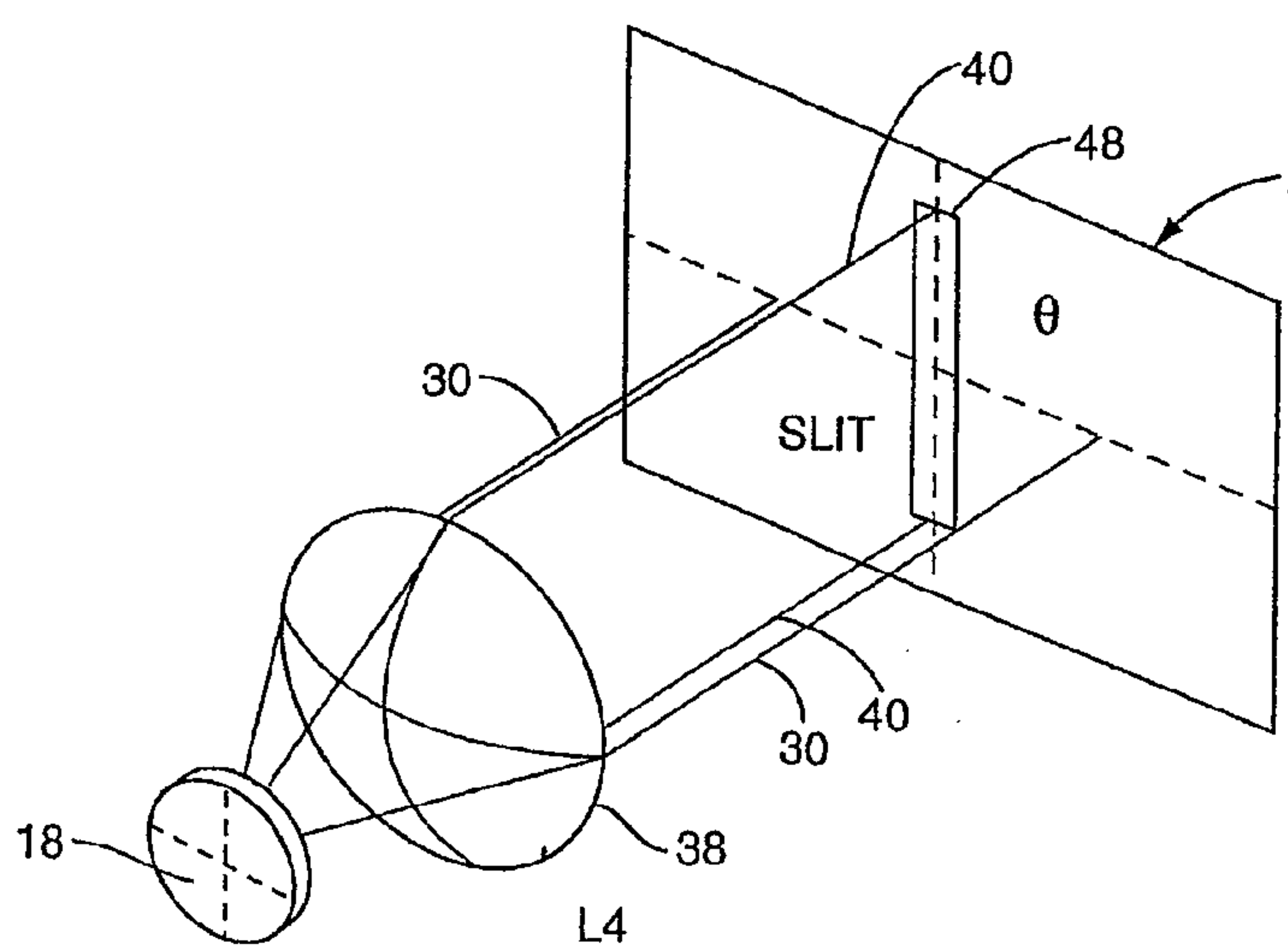
40
48
28
θ
30
SLIT
40
30
18
38
L4
SAMPLE

FIG. 1B

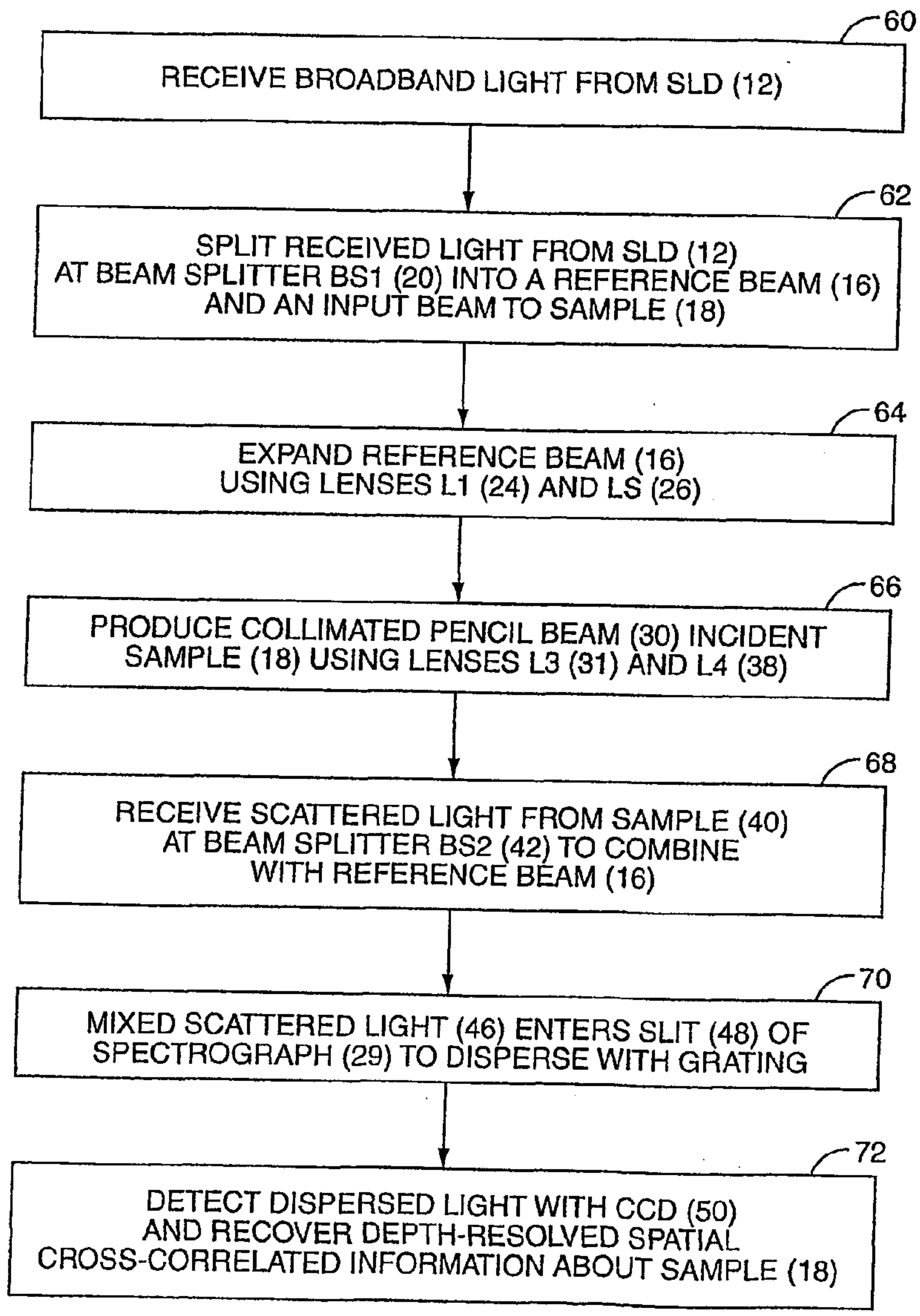
60
RECEIVE BROADBAND LIGHT FROM SLD (12)
62
SPLIT RECEIVED LIGHT FROM SLD (12) AT BEAM SPLITTER BS1 (20) INTO A REFERENCE BEAM (16) AND AN INPUT BEAM TO SAMPLE (18)
64
EXPAND REFERENCE BEAM (16) USING LENSES L1 (24) AND LS (26)
66
PRODUCE COLLIMATED PENCIL BEAM (30) INCIDENT SAMPLE (18) USING LENSES L3 (31) AND L4 (38)
68
RECEIVE SCATTERED LIGHT FROM SAMPLE (40) AT BEAM SPLITTER BS2 (42) TO COMBINE WITH REFERENCE BEAM (16)
70
MIXED SCATTERED LIGHT (46) ENTERS SLIT (48) OF SPECTROGRAPH (29) TO DISPERSE WITH GRATING
72
DETECT DISPERSED LIGHT WITH CCD (50) AND RECOVER DEPTH-RESOLVED SPATIAL CROSS-CORRELATED INFORMATION ABOUT SAMPLE (18)

FIG. 2

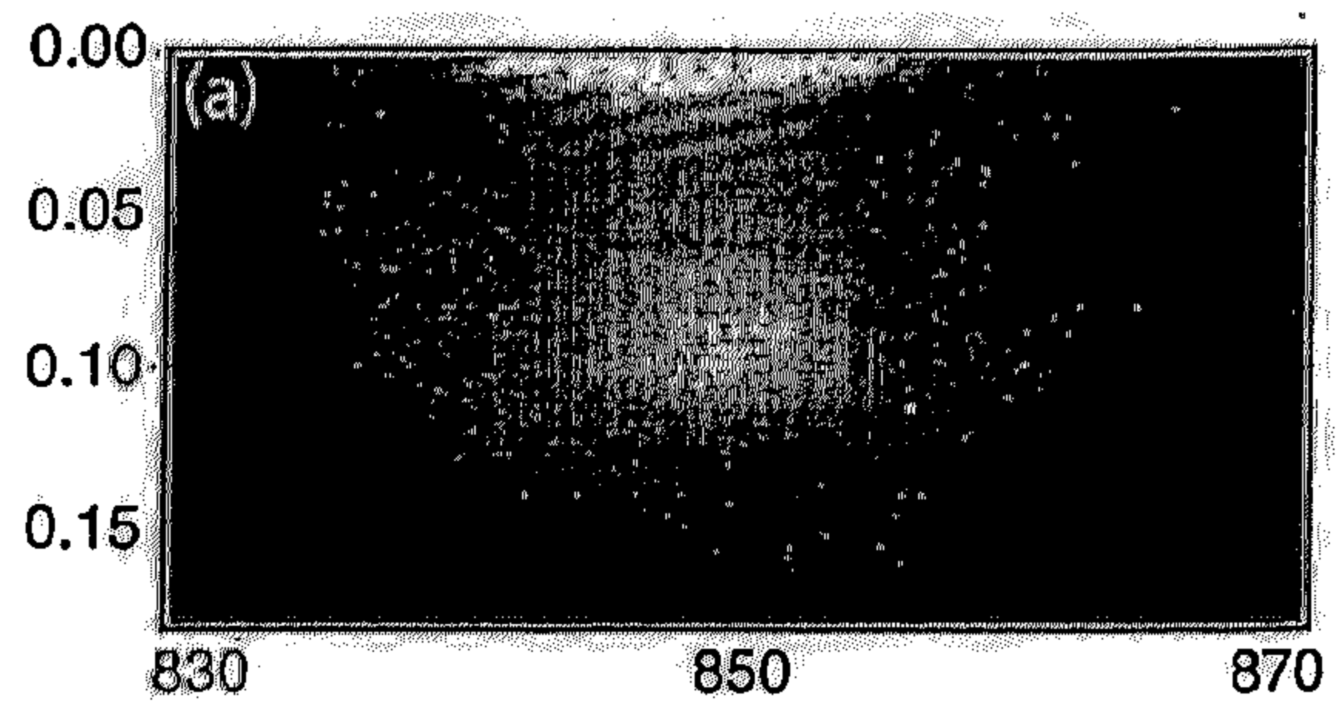

FIG. 3A

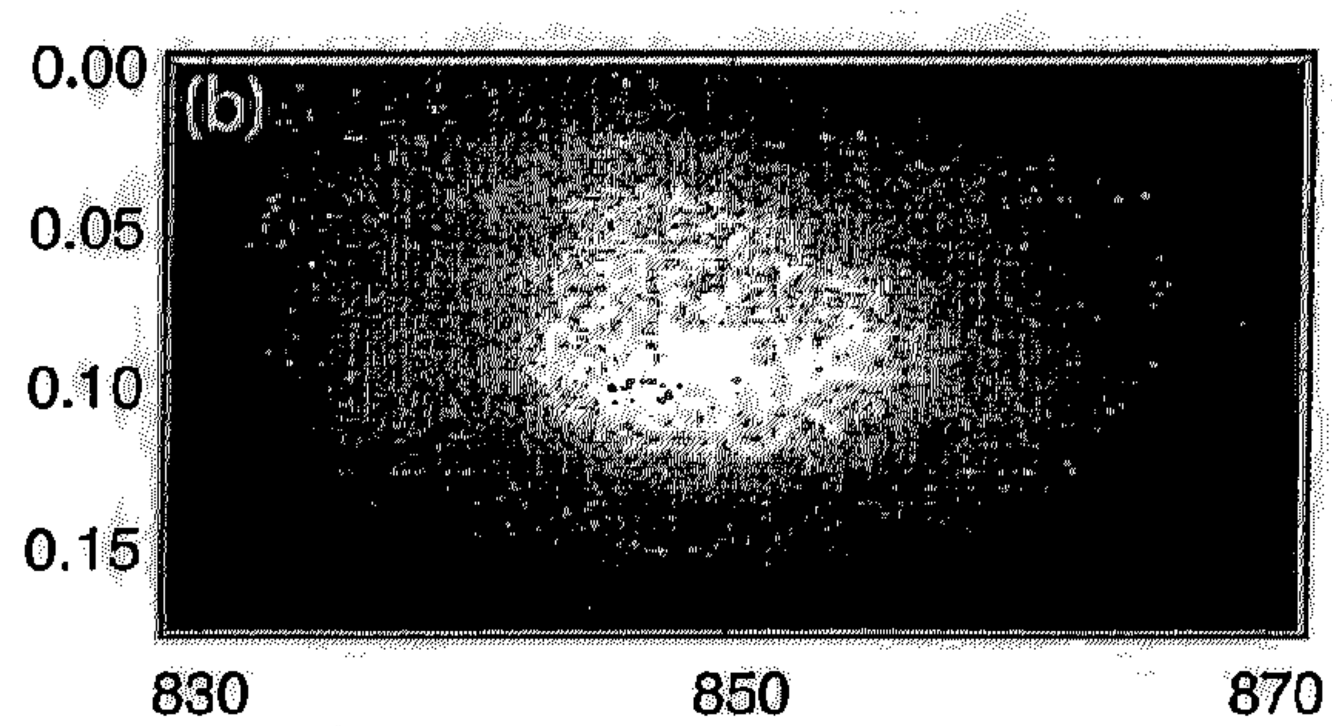

FIG. 3B

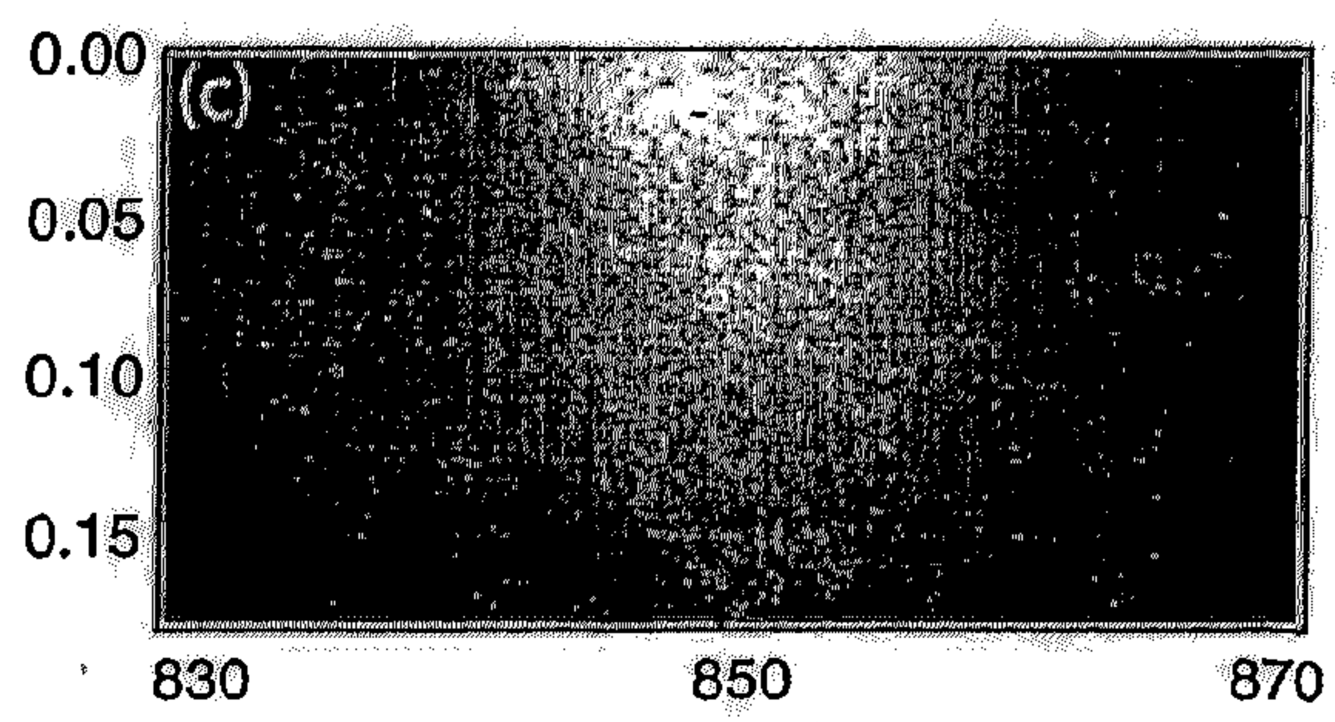

FIG. 3C

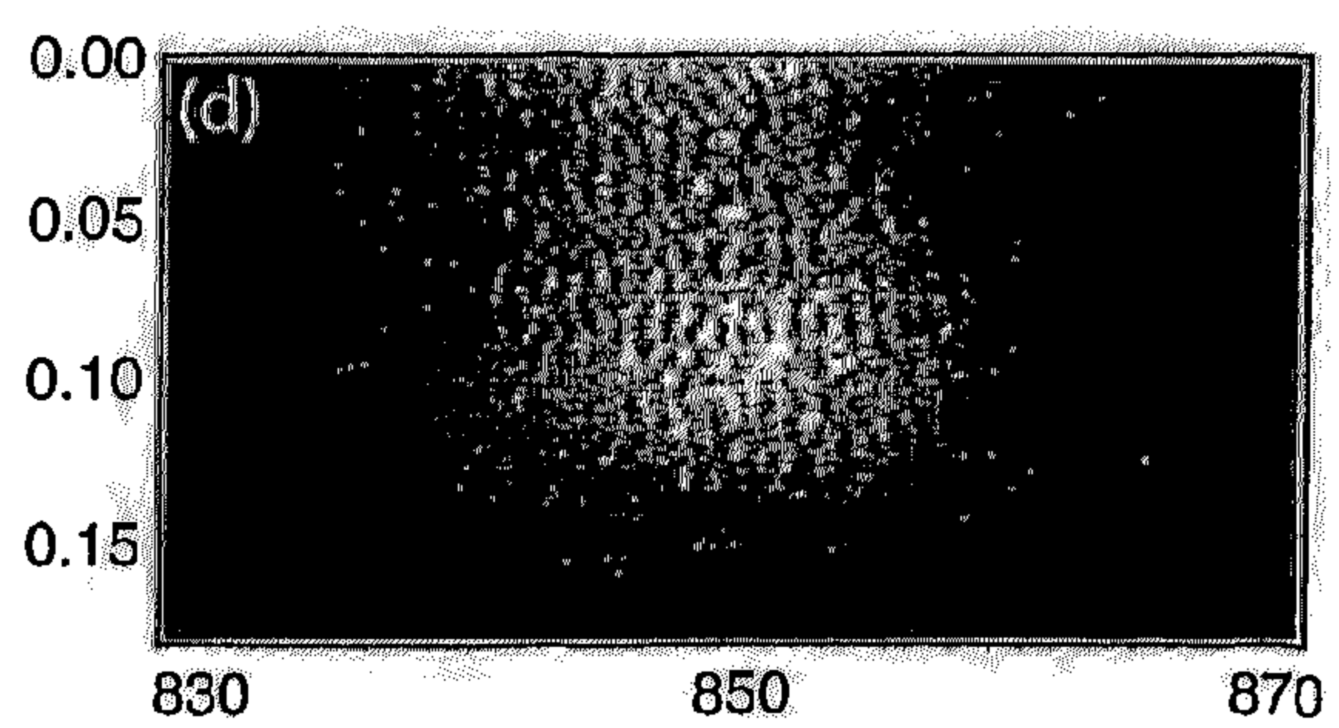

FIG. 3D

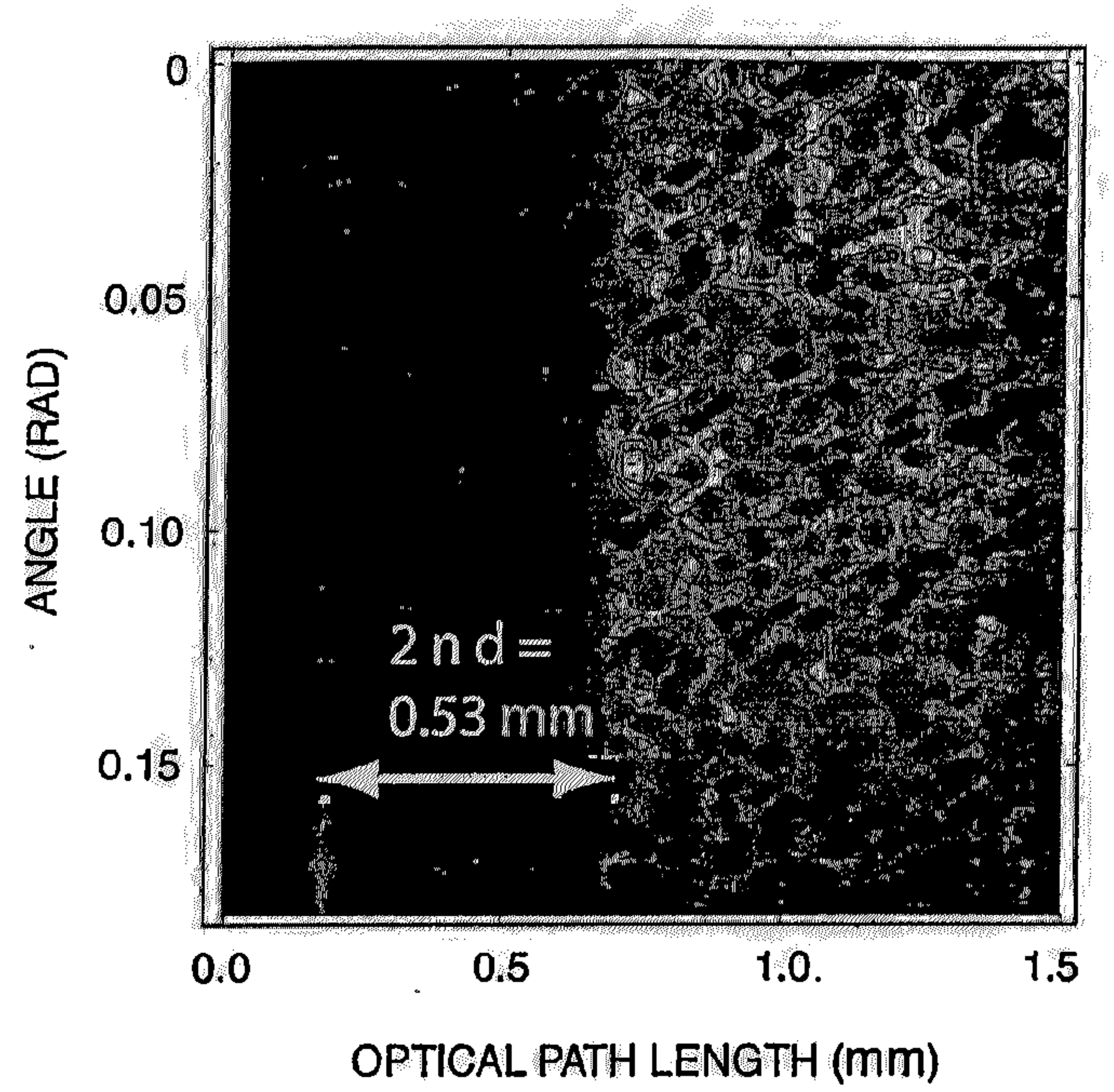
0
0.05
0.10
0.15
ANGLE (RAD)
2nd=
0.53 mm
0.0
0.5
1.0
1.5
OPTICAL PATH LENGTH (mm)

FIG. 4A

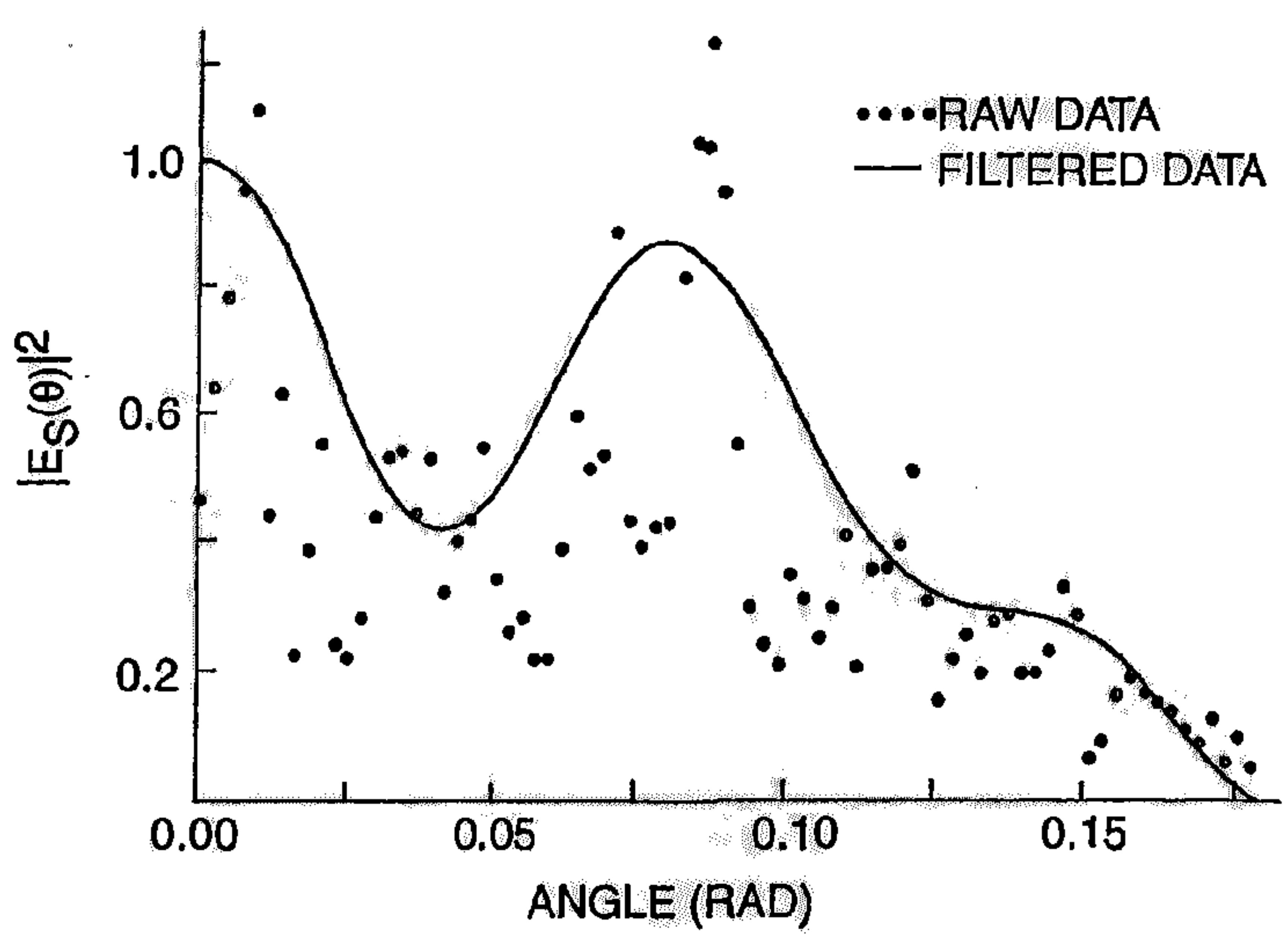
RAW DATA
FILTERED DATA
1.0
0.6
0.2
$|E_S(\theta)|^2$
0.00
0.05
0.10
0.15
ANGLE (RAD)

FIG. 4B

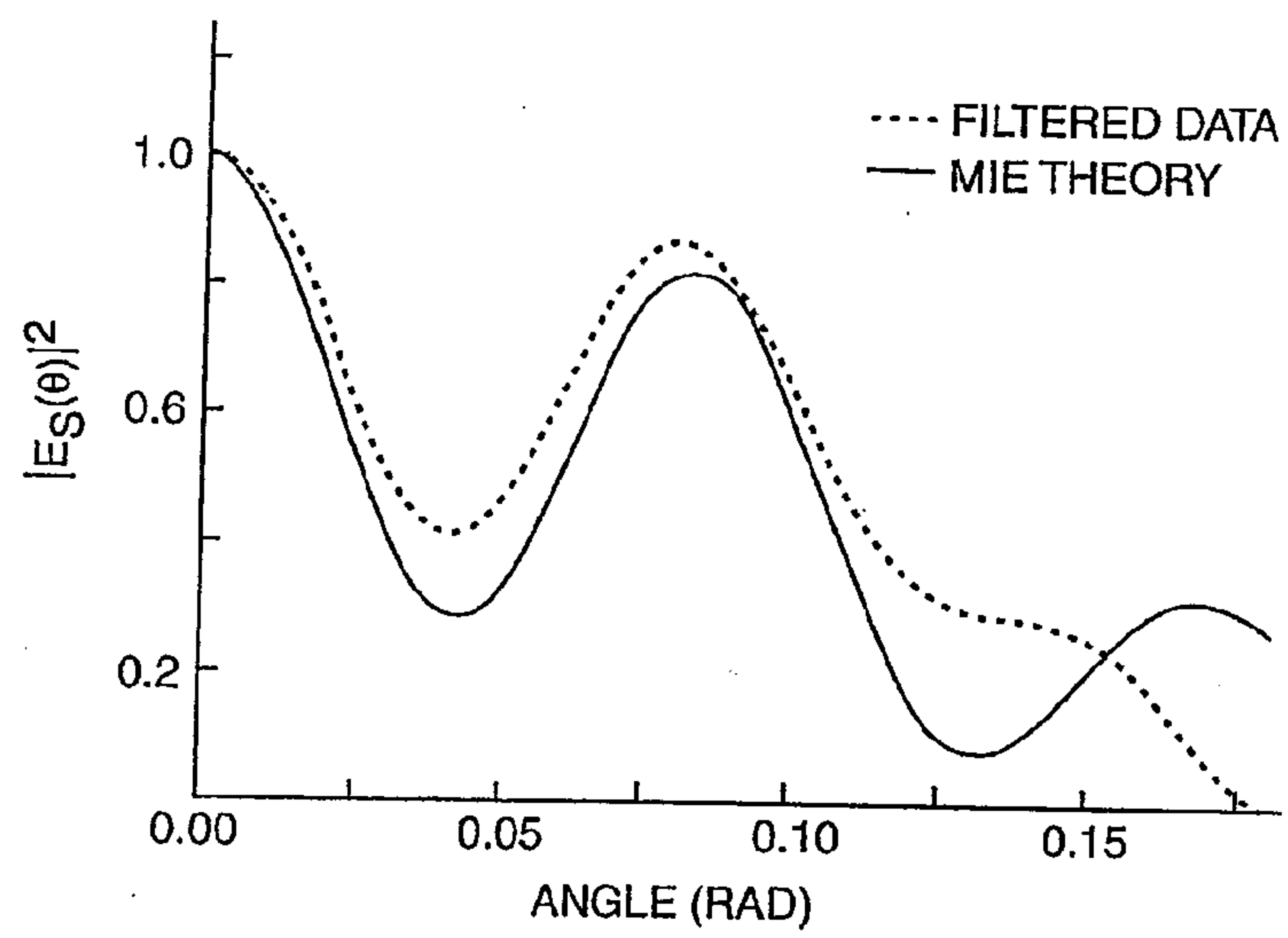
FILTERED DATA
MIE THEORY
1.0
0.6
0.2
$|E_S(\theta)|^2$
0.00
0.05
0.10
0.15
ANGLE (RAD)

FIG. 5A

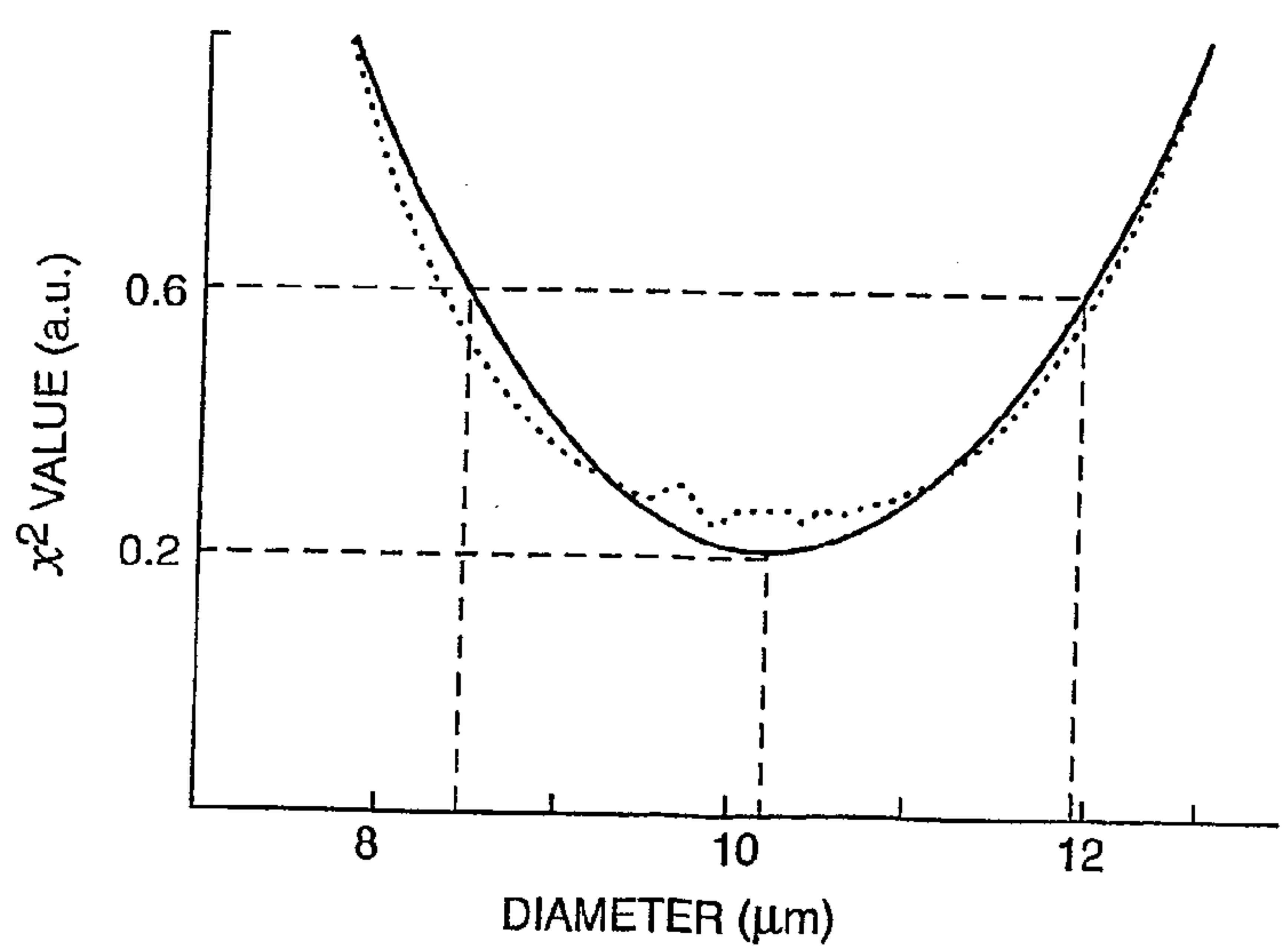
0.6
0.2
χ^2 VALUE (a.u.)
8
10
12
DIAMETER (μm)

FIG. 5B

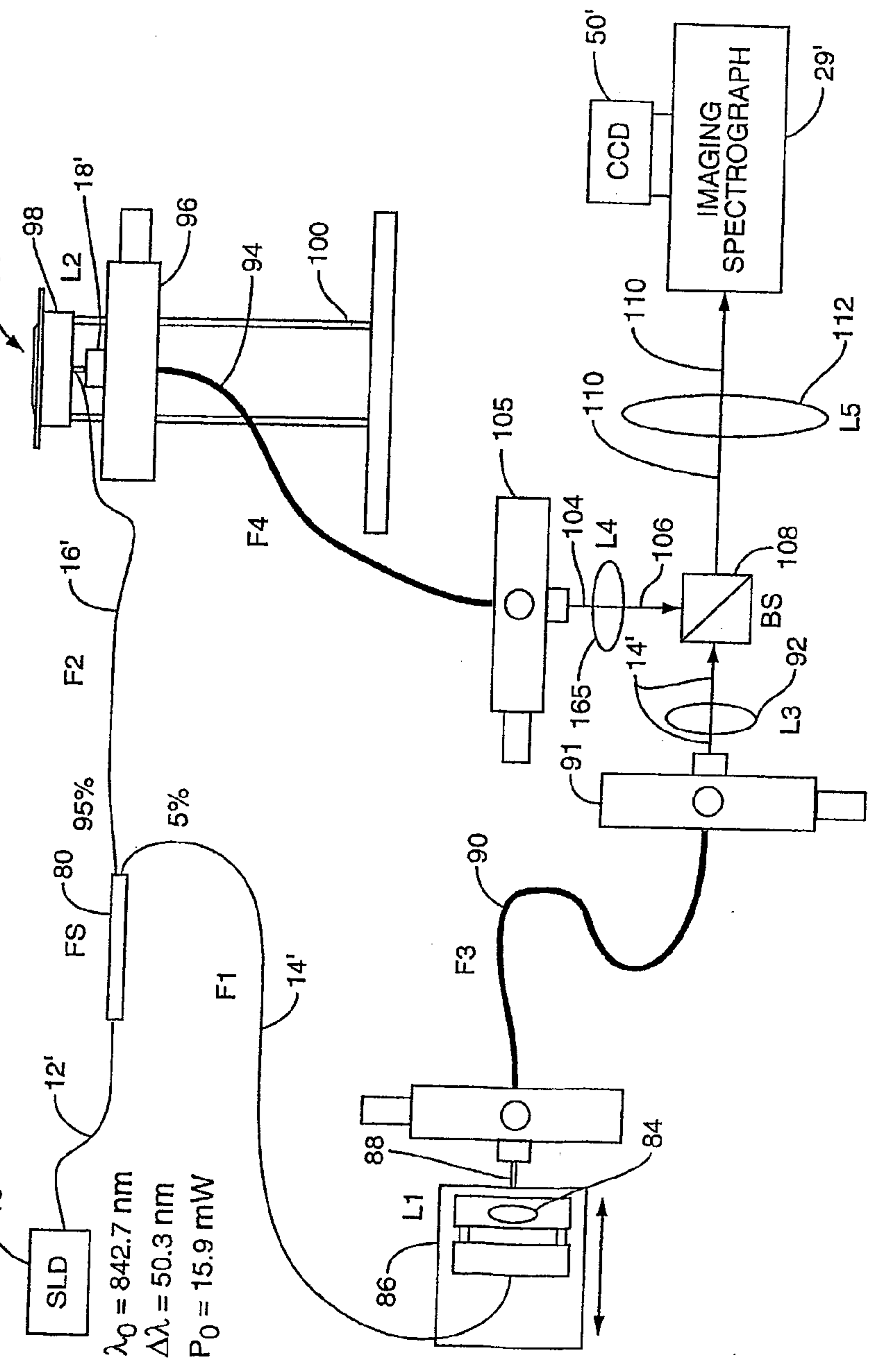
SLD
10'
λ0 = 842.7 nm
Δλ = 50.3 nm
P0 = 15.9 mW
12'
FS
80
95%
5%
F1
14'
F2
16'
18'
L2
98
82
96
94
100
F4
105
104
L4
106
BS
108
165
14'
92
L3
91
90
F3
88
84
L1
86
CCD
50'
IMAGING SPECTROGRAPH
29'
110
110
110
112
L5

FIG. 6

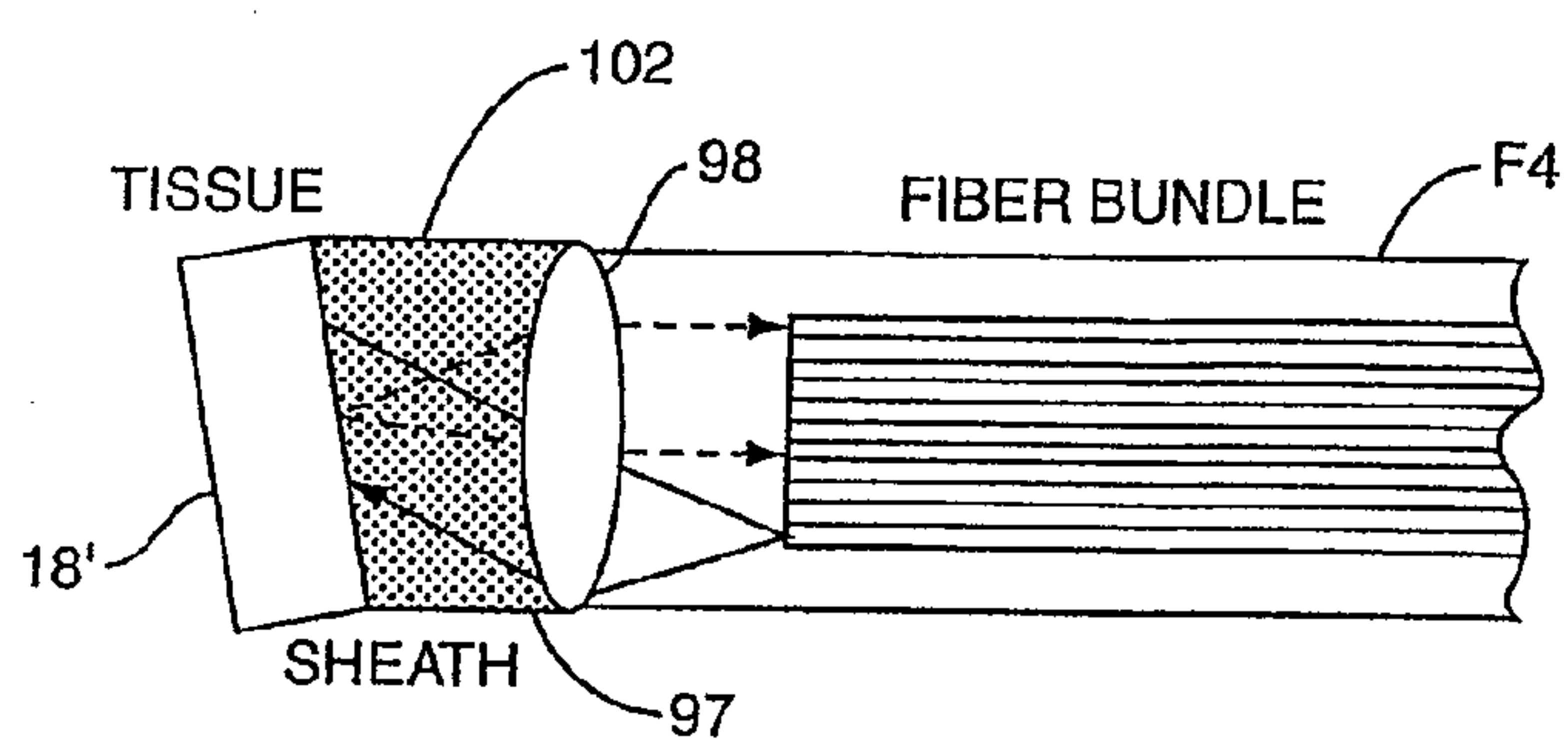
102
TISSUE
98
FIBER BUNDLE
F4
18'
SHEATH
97

FIG. 7A

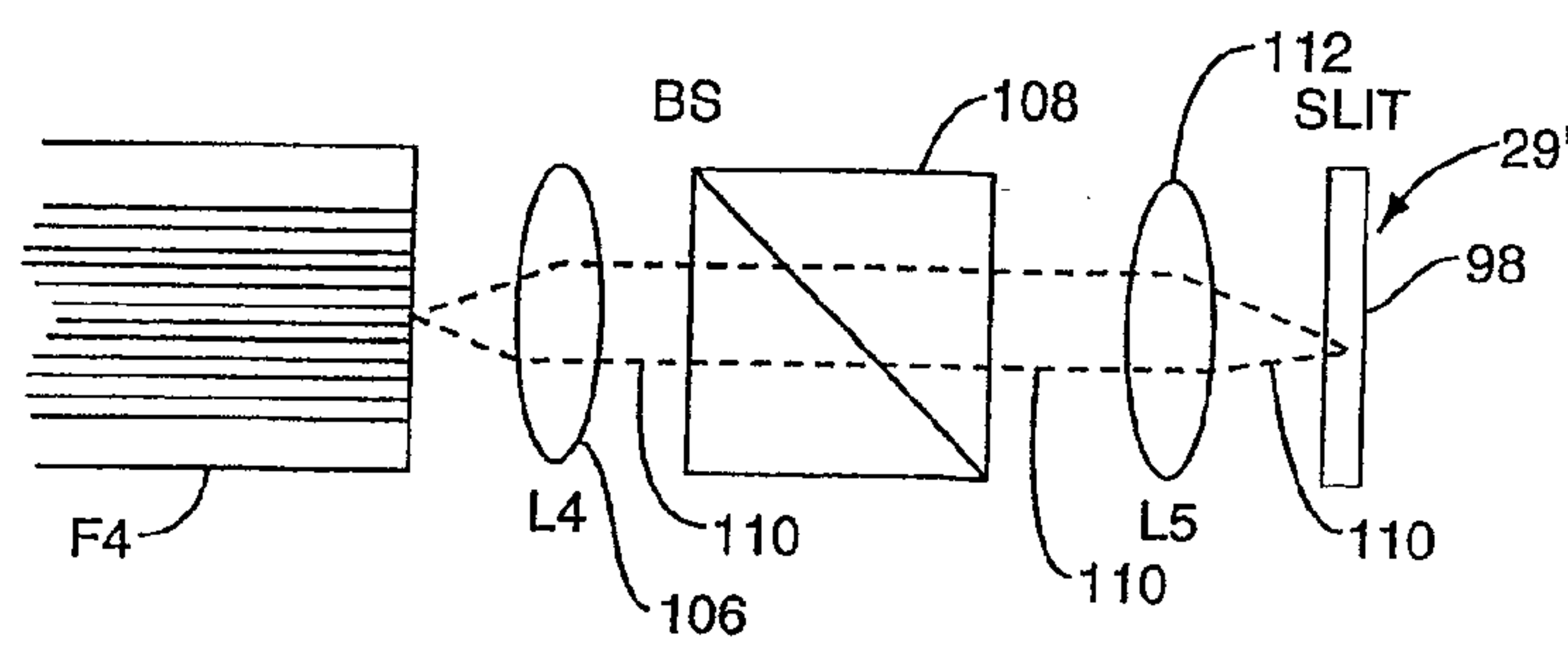
112
SLIT
BS
108
29'
98
F4
L4
110
106
110
L5
110

FIG. 7B

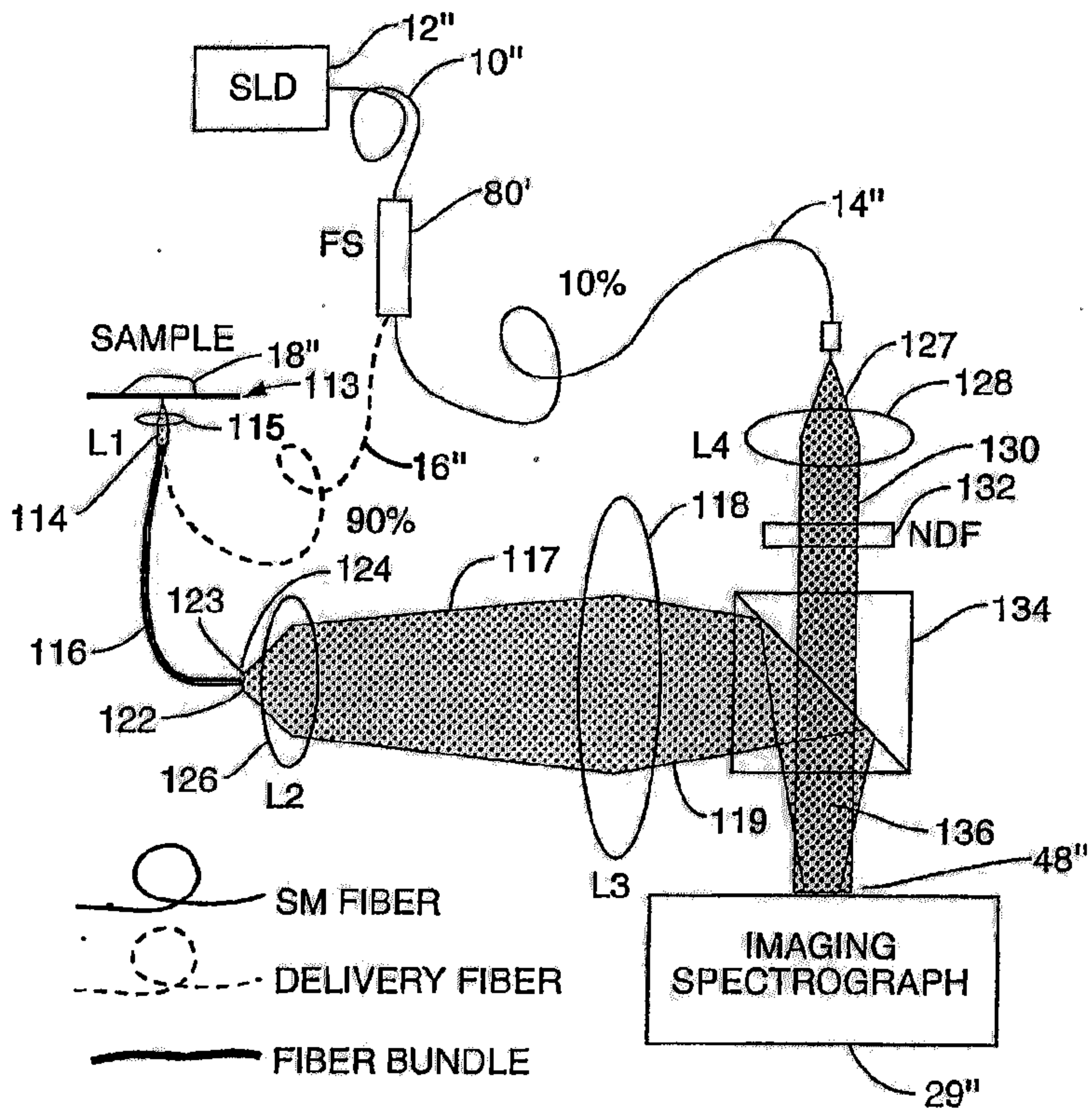

FIG. 8A

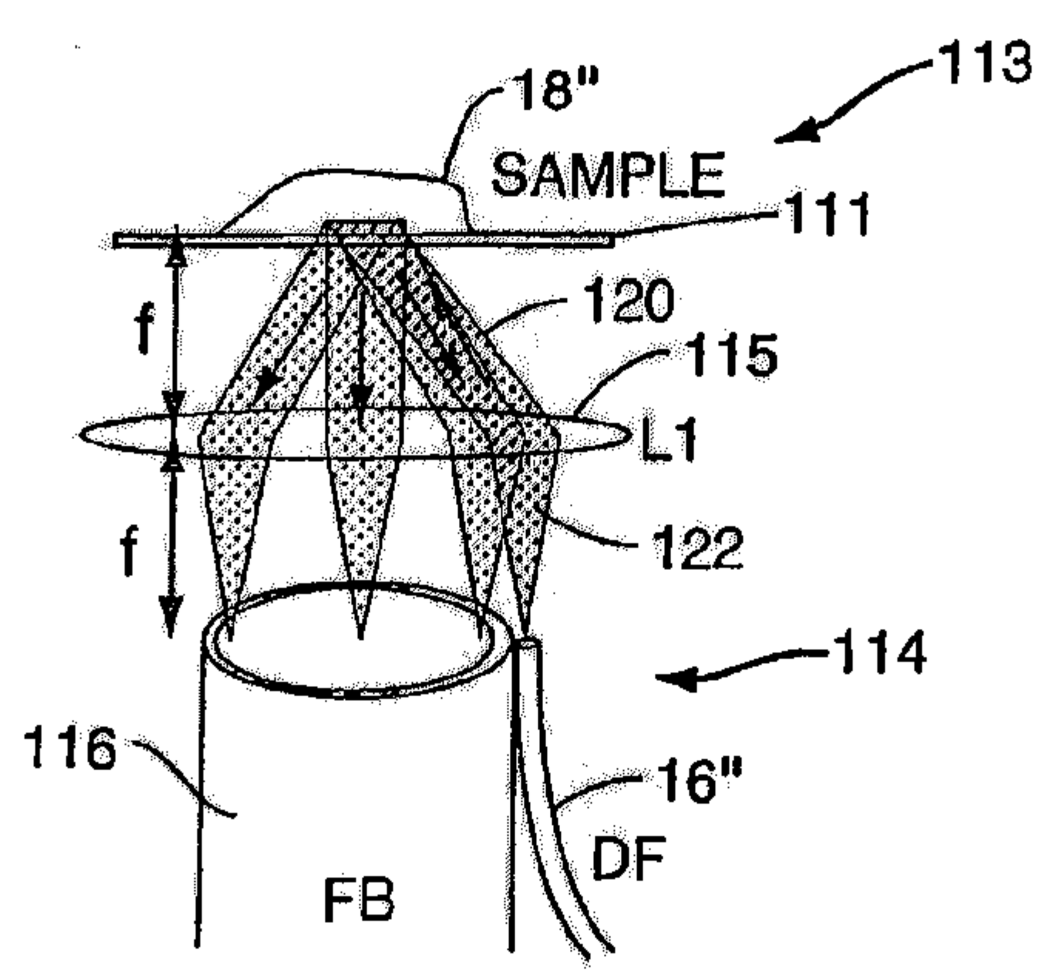

FIG. 8B

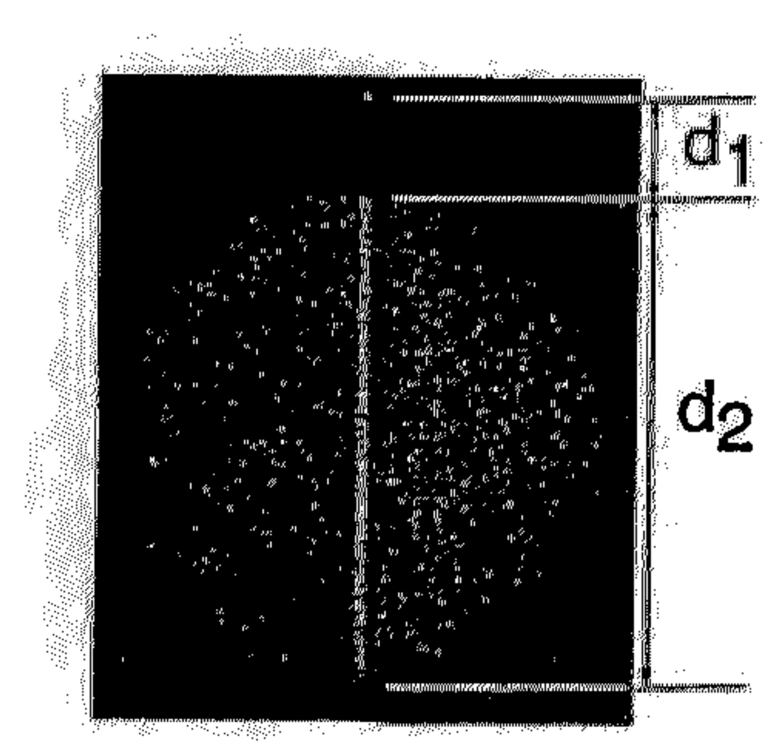

FIG. 8C

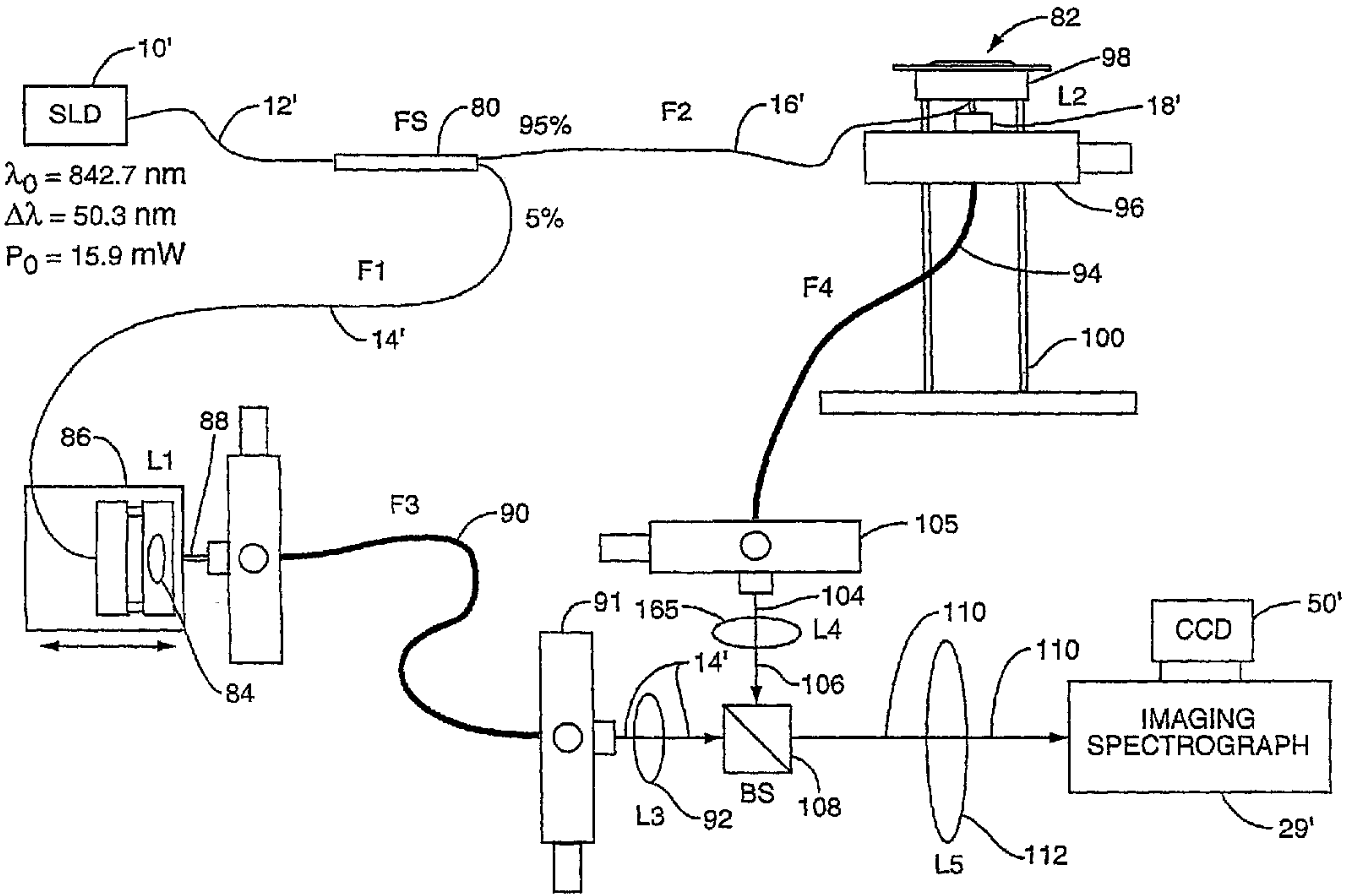

SLD
10'
12'
FS
80
95%
F2
16'
82
98
L2
18'
96
$\lambda_0 = 842.7$ nm
$\Delta\lambda = 50.3$ nm
$P_0 = 15.9$ mW
5%
F1
14'
F4
94
100
86
L1
88
84
F3
90
105
104
91
165
L4
14'
106
110
110
CCD
50'
IMAGING SPECTROGRAPH
29'
L3
92
BS
108
L5
112